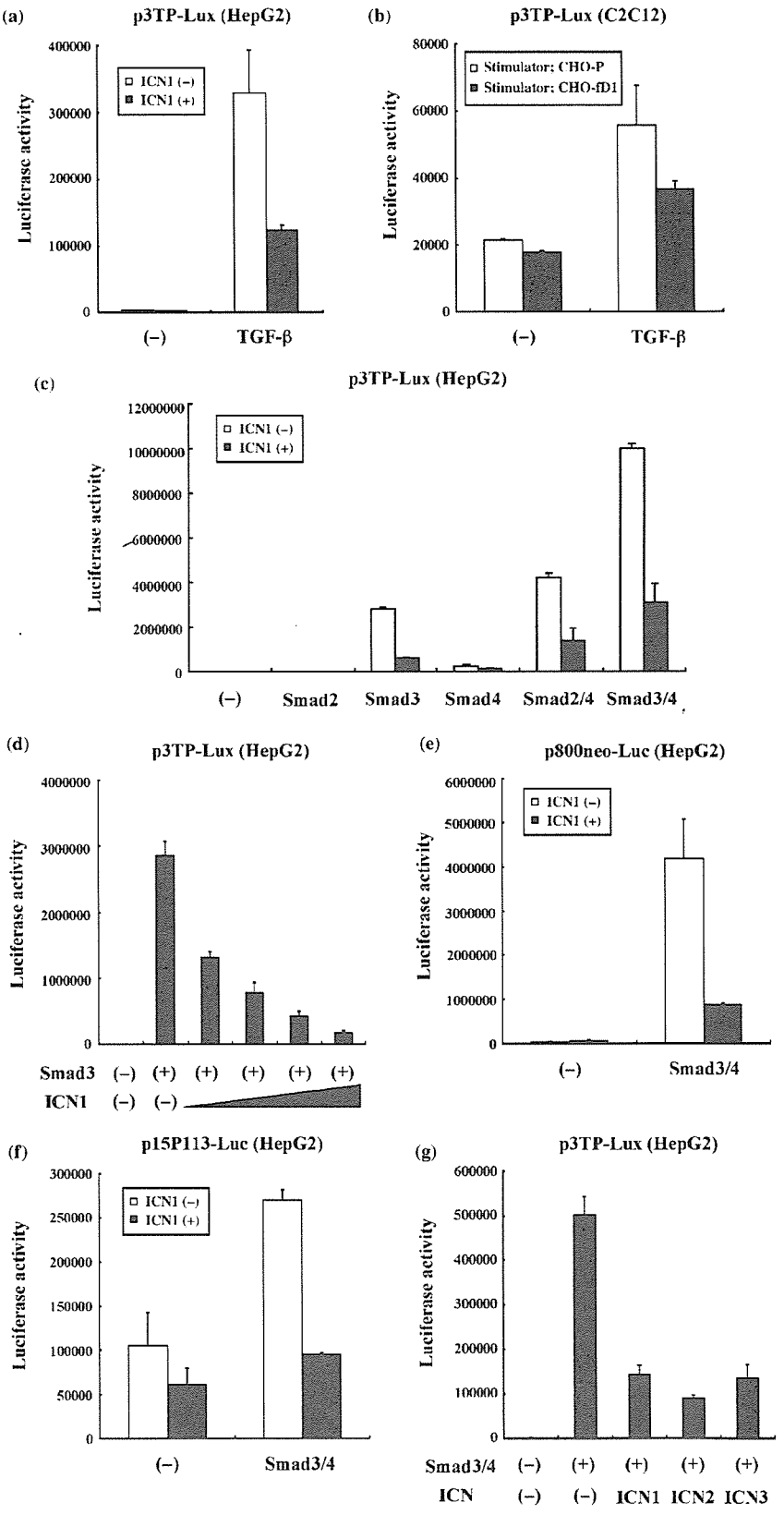

Fig. 3. Transforming growth factor (TGF)-β or Smad-mediated transcriptional responses are suppressed by Notch signaling. (a) TGF-β-induced transcriptional responses are repressed by ICN1. p3TP-Lux was transfected into HepG2 cells together with either pcDNA3 empty vector or pcDNA3-ICN1. Cells were incubated in the absence or presence of 1 ng/mL TGF-β for 48 h, and luciferase activities were measured. (b) Notch ligand stimulation also inhibits the TGF-β-mediated transcriptional responses. C2C12 cells, transiently transfected with p3TP-Lux, were cocultured with either irradiated parental CHO(r) cells (CHO-P) or irradiated CHO(r) cells expressing full-length Delta1 (CHO-fD1) in the absence or presence of 5 ng/mL TGF-β for 48 h, and luciferase activities were measured. (c) ICN-1 suppresses Smad-induced transcriptional responses. Either pcDNA3 empty vector or pcDNA3-ICN1, together with p3TP-Lux, was transfected into HepG2 cells, in combination with the indicated Smad constructs. (d) ICN1 represses Smad-induced responses in a dose-dependent manner. HepG2 cells were transfected with 3, 10, 30 or 100 ng ICN1 expression plasmid, together with p3TP-Lux and Smad3. Smad-induced transcriptional responses with (e) p800neo-Luc or (f) p15P113-Luc are also repressed by ICN1. p800neo-Luc or p15P113-Luc was transfected into HepG2 cells together with either pcDNA3 empty vector or pcDNA3-ICN1, in combination with Smad3 and Smad4. (g) ICN2 and ICN3 suppress the Smad-mediated transcriptional activation as ICN1. Either pTracerCMV empty vector, pTracerCMV/ICN1, pTracerCMV/ICN2 or pTracerCMV/ICN3 was transfected into HepG2 cells, together with p3TP-Lux, Smad3 and Smad4, and luciferase activities were measured.

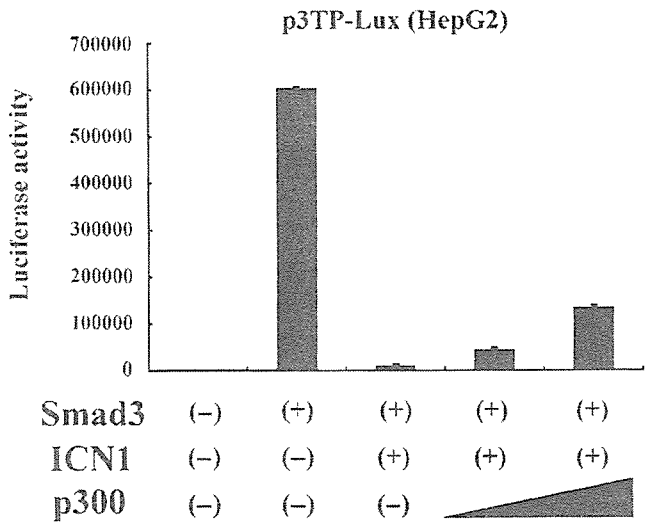

Fig. 4. Repression of Smad3-mediated transactivation by ICN1 is recovered with coactivator p300. Introduction of p300 partially rescues the ICN1-mediated suppression of Smad3-induced p3TP-Lux transactivation in a dose-dependent manner. HepG2 cells were transfected with 0.1 or 1 μg p300 expression plasmid, together with p3TP-Lux, Smad3 and ICN1, followed by a luciferase assay.

with or without the p300 interaction capability (Fig. 5a). RAMICΔC is a C-terminally truncated mutant that lacks the TAD and PEST domains but contains the EP domain. In RAM/ANK, the EP domain and all the sequence C-terminal to it are deleted. ΔEP is an internal deletion mutant lacking only 15 amino acids corresponding to the EP domain. EP (LDE/AAA) carries a three-amino acid substitution, i.e. LDE to AAA within the EP domain, which was previously demonstrated to be critical for transactivation of Notch signaling as well as for the interaction with p300.[22] As expected, RAM/ANK, ΔEP and EP (LDE/AAA), all of which lose the capacity to interact with p300, failed to fully repress transcription from the 3TP promoter induced by overexpression of Smad3 and Smad4. In contrast, RAMICΔC, which binds to p300, suppressed the TGF-β/Smad-induced transactivation just as wild-type ICN1 did (Fig. 5b). The expression levels of ICN1 and its derivatives in HepG2 cells were analyzed by Western blotting (Fig. 5b). These results suggest that the EP domain is required for the suppression of the Smad transactivation by ICN1.

ICN1 reduces the amount of p300 binding to Smad3. To determine whether ICN1 interferes with Smad3 activity through sequestration of p300, we investigated the effect of wild type and various mutants of ICN1 on the interaction between Smad3 and p300 in the presence of activated TGF-β receptor. As shown in previous reports,[24] we observed that Smad3 was coimmunoprecipitated with p300 (Fig. 6). The amount of coimmunoprecipitated Smad3, however, was markedly reduced when wild-type ICN1 was cotransfected. RAMICΔC showed a similar effect, whereas RAM/ANK, ΔEP and EP (LDE/AAA) had little or no effect on the amounts of Smad3 coprecipitated with p300 (Fig. 6). Taken together, these results suggest that the EP domain of ICN1 is essential for the sequestration of p300 from Smad3.

The RBP-J-dependent transcription of target genes is not required for the repression of TGF-β signaling by ICN1. If the inhibition of Smad3-mediated transcriptional activation by ICN1 is attributed

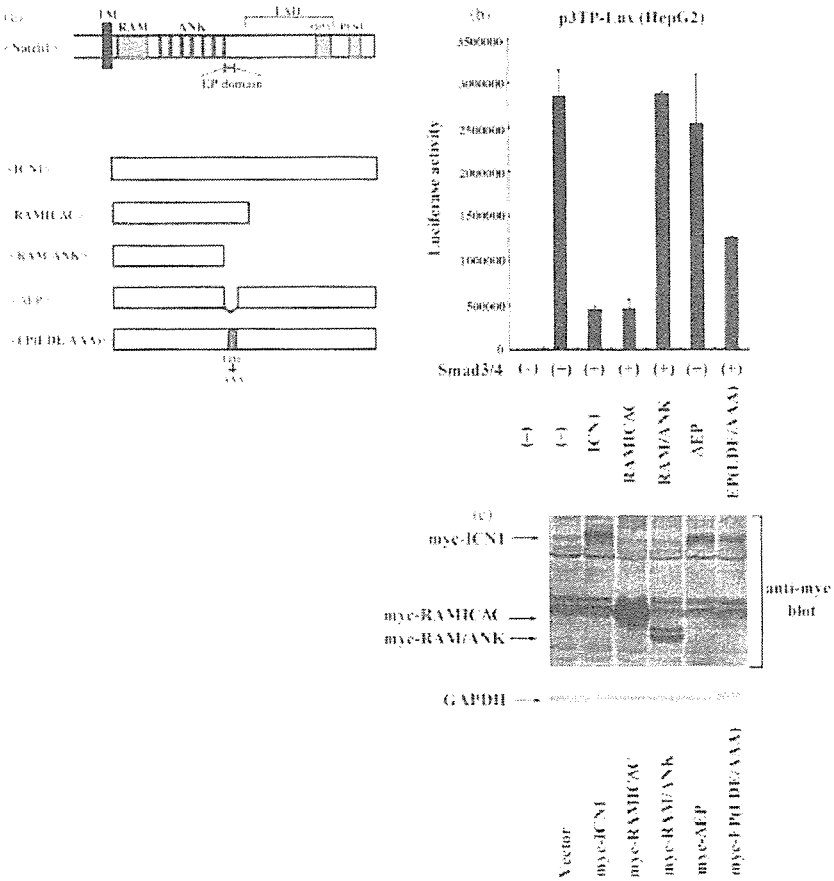

Fig. 5. The EP domain is indispensable for suppression of Smad signaling by ICN1. (a) Schematic representation of the mouse Notch1 intracellular region (ICN1) and its derivatives used in this study. The EP domain, essential for ICN1 to interact with p300, is located in the C-terminal flanking region adjacent to the ankyrin repeats of ICN1. (b) Structural requirements for repression of Smad signaling by ICN1. HepG2 cells were transfected with Smad3, Smad4 and p3TP-Lux together with wild type or each mutant of ICN1, and luciferase activities were measured. Expression levels of myc-ICN1 and its myc-tagged derivatives were evaluated in HepG2 cells. Each whole cell extract was analyzed by Western blotting using an anti-myc antibody (upper panel). The lower panel shows the glyceraldehyde-3-phosphate dehydrogenase expression as loading control.

 doi: 10.1111/j.1349-7006.2005.00048.x

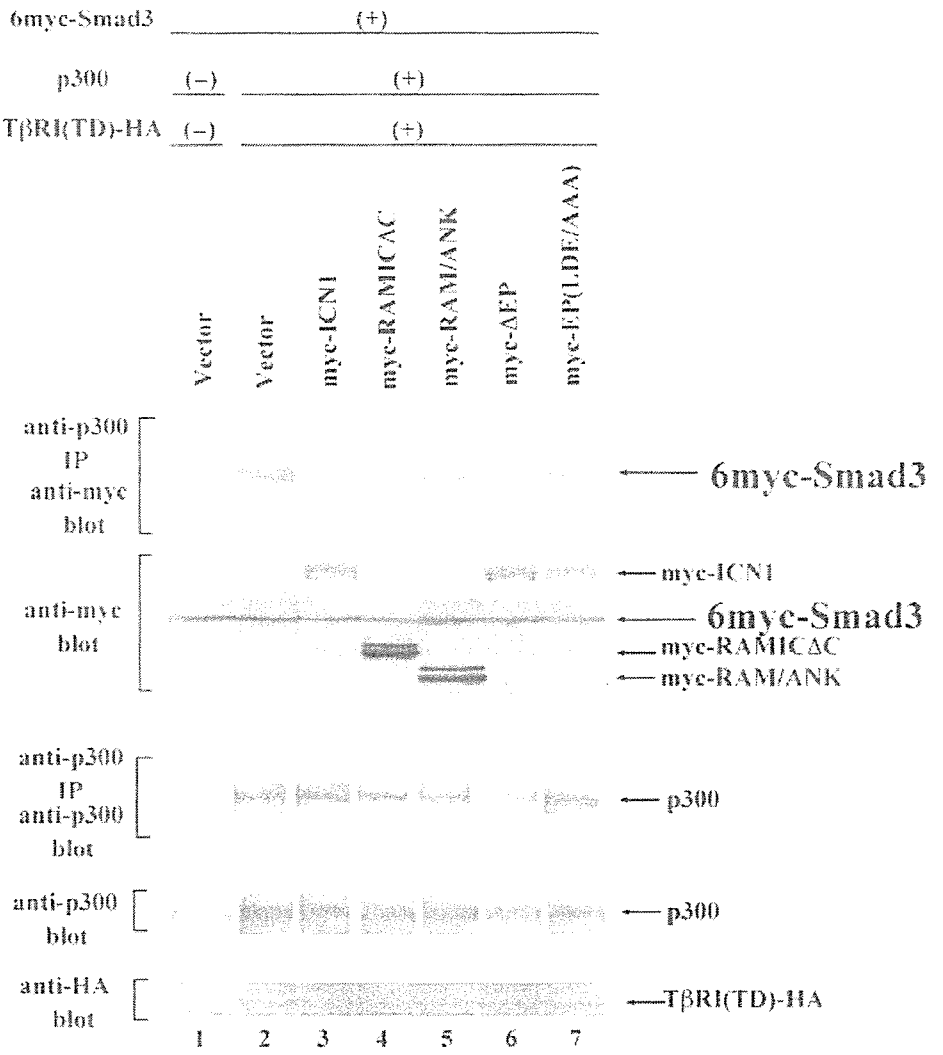

Fig. 6. Effects of ICN1 on the p300–Smad interaction. Wild type or each mutant of ICN1 was coexpressed in COS-7 cells with 6myc-Smad3, TβRI(TD)-HA and p300. The cell lysates of transfected COS-7 cells were subjected to immunoprecipitation with anti-p300 antibody followed by immunoblotting with anti-myc antibody, which detects the interaction of p300 and 6myc-Smad3. Immunoprecipitates were also blotted with anti-p300 antibody, and cell lysates were blotted with anti-myc, anti-p300 and anti-hemagglutinin A antibodies.

to the sequestration of p300 from Smad3, we hypothesized that it may not be mediated by transcription targeted by the complex of ICN1 and RBP-J (or CSL from *C*BF1/RBP-J, *S*uppressor of Hairless, *L*ag-1), a DNA-binding protein with which activated Notch proteins transactivate target genes. To clarify this possibility, we used a dominant-negative form of RBP-J (RBP-J [R218H];[40] hereafter referred to as DN-RBP), which lacks the ability to bind to DNA but still interacts with Notch1 and represses ICN1-induced transactivation of the TP-1 promoter (Fig. 7a). Reporter assays showed that DN-RBP did not reverse the ICN1-induced repression of TGF-β signaling, indicating that the RBP-J-dependent transcription of specific target genes is not required for ICN1-induced repression of TGF-β signaling (Fig. 7b).

Discussion

In this study, we have demonstrated a transcriptional cross-talk between the Notch and TGF-β signaling pathways. Because Smad proteins are important tumor suppressors, the ability of active Notch1 (ICN1) to repress TGF-β signaling could be responsible, at least partially, for the transforming activity of Notch. A recent study has reported that ICN1 blocks TGF-β-mediated growth arrest in epithelial cells.[41] In that context, ICN1 deregulates expression of c-Myc and thereby renders epithelial cells resistant to growth-inhibitory signals, suggesting a novel link between Notch and cell cycle control. In the experiments described here, we show another mechanism explaining the antagonism between the Notch and TGF-β signaling systems, that is, repression of TGF-β-mediated signaling through sequestration of coactivator p300 by ICN1, which is apparently independent from the mechanism demonstrated by Rao and Kadesch.[41]

Importantly, some investigators have demonstrated that Notch and Smad signaling show functional synergism.[42–44] More complexly, transcriptional activation of the hairy/enhancer of split (HES)-related gene Hey1 is both a direct target of Smad3 and an indirect target through Smad3-dependent transcriptional activation of Notch signaling component genes.[45] Demonstration of direct and TGF-β-dependent interactions between Smad3 and ICN1,[44] and Smad1/5 and ICN1,[42,43] indeed serves as bona-fide evidence of the cross-talk between these two signaling

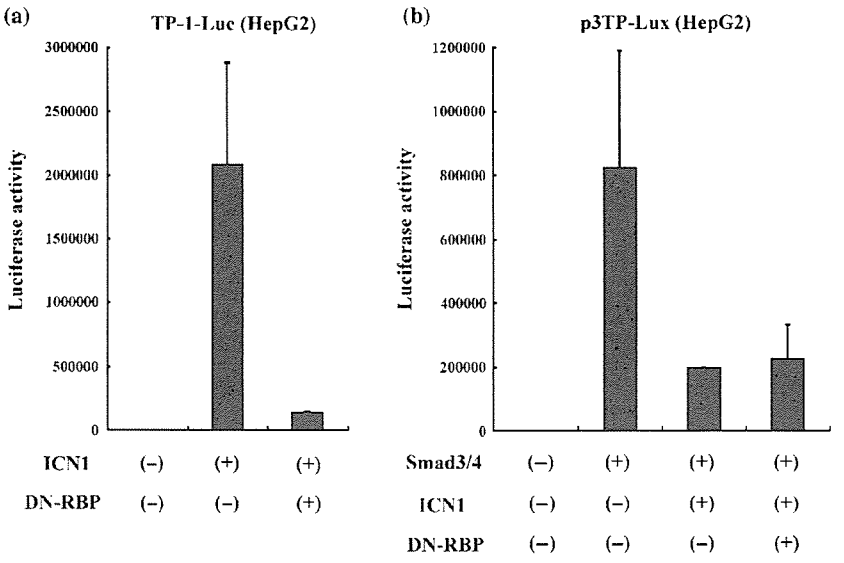

Fig. 7. The effects of DN-RBP on the transcriptional activity of ICN1 and the Smad proteins. (a) Expression of a dominant-negative form of RBP-J (DN-RBP) suppresses TP-1 activity induced by ICN1. TP-1-Luc was transfected into HepG2 cells, together with ICN1 and DN-RBP. (b) DN-RBP does not reverse the ICN1-induced repression of the Smad signaling. p3TP-Lux was transfected into HepG2 cells, together with Smad3, Smad4, ICN1 and DN-RBP.

systems. It appears that various molecular interactions could exist between these two signaling systems, most likely in a cell context-dependent manner. Indeed, there is a report showing that both synergy and antagonism could occur between the Notch and Smad signaling systems.[43]

Many transcription factors, including ICN1 and Smads, use the coactivator p300 to activate transcription.[22–24] The p300 protein is generally present at limiting concentrations within the cell nucleus, and functional antagonism between transcription factors occurs as a consequence of direct competition for binding to p300.[46–50] Domains within the p300 protein for interaction with individual transcription factors are highly variable, but both active Notch1 and Smad have been reported to bind to the C-terminal domain, which can potentially be shared. Our results suggest competition between active Notch1 and Smad for limiting quantities of complexes containing p300. Similar competition for p300 has been described for several cellular pathways, including nuclear receptor and AP-1,[46] p53 and E2F,[47] NF-κB and p53,[48] NF-κB and nuclear receptor,[49] and STAT and AP-1.[50]

Regarding Notch-induced transformation, previous studies have indicated that in baby rat kidney cells (RKE) immortalized with E1A, the minimal transforming domain includes ANK and flanking 107 C-terminal amino acids.[15] Consistent with this, our data showed that the EP domain, adjacent to ANK, is required for suppressing Smad activity by ICN1. Recently, the crystal structure revealed that the LDE motif in the EP domain not only governs the stability around this domain but also potentially contributes to direct contacts with p300,[51] supporting our result that the EP mutant (LDE/AAA) fails to sequester p300 from Smad3. Moreover, it is interesting that p300 was isolated as a cellular target of the adenoviral oncoprotein E1A,[52] which is known to block the functions of p300. Therefore, we can speculate that ICN1 may promote sequestration of p300 from Smad3 in cooperation with E1A in RKE cells.

In this study, the biological phenomenon under this transcriptional cross-talk was assessed by both upregulation and downregulation of Notch signaling. For the former, we used strategies of ligand stimulation and overexpression of constitutively active Notch1. For the latter, siRNA-based suppression of Notch1 synthesis in CaSki cells was used successfully to significantly reduce spontaneous generation of the cleaved (i.e. active form of) Notch1. We can speculate that Notch1 is spontaneously activated in CaSki cells either by ligand stimulation from neighboring cells or a cell-autonomous mechanism. In either case, we have demonstrated that spontaneous activation of Notch1 contributes to the growth of CaSki cells, and that blockade of this activation results in a recovered responsiveness to TGF-β. Taken together, we have here demonstrated that active Notch1 may serve as a positive regulator of cell growth by repressing TGF-β-induced growth inhibition. We observed, however, that CaSki cells made no response to TGF-β under treatment with γ-secretase inhibitors, chemical compounds that block Notch cleavage, despite our observation that the amount of active Notch1 was decreased and the transcriptional activation of the Notch reporter gene was suppressed when CaSki cells were treated with γ-secretase inhibitors (data not shown). This observation was apparently puzzling. However, it has since been reported that many transmembrane proteins, in addition to Notch and the amyloid precursor protein that was the substrate identified originally, could be substrates of the γ-secretase.[53] These new lines of evidence made it possible for us to speculate that γ-secretase inhibitors might influence other growth signal pathways and that the specific knockdown of Notch signaling might be achieved using the RNA interference technique, rather than with a γ-secretase inhibitor. It is of future interest to elucidate the mechanisms underlying the failure to restore responsiveness to TGF-β by γ-secretase inhibitors in CaSki cells.

Genetic and molecular studies have implicated several downstream components in the Notch signaling pathway, such as RBP-J and Deltex. As RBP-J is one of the main effectors in Notch signaling,[37,54] it is critical to determine whether the RBP-J-dependent transcription is required for the inhibitory effect of Notch signaling. If that is the case, DN-RBP, a DNA-binding mutant that perturbs Notch activity in a dominant-negative manner, should cancel this suppression. The negative result of the experiment using DN-RBP, however, suggests that RBP-J-dependent transcription of specific target genes is not required for the inhibition of TGF-β signaling.

The p300 protein functions as global transcriptional coactivator and plays important roles in a broad spectrum of biological processes, including cell proliferation and differentiation.[52] A role for p300 in tumor suppression has been proposed, and biallelic mutations of p300 have been identified in certain types of human cancers.[55,56] Furthermore, it was reported recently that reintroduction of wild-type p300 suppresses the growth of p300-deficient carcinoma cells.[57] Insufficiency of cyclic AMP response element binding protein (CBP), a coactivator closely

 doi: 10.1111/j.1349-7006.2005.00048.x

related to p300, also results in both Rubinstein–Taybi Syndrome in humans, a disease characterized by an increased propensity for malignancies, and an increased incidence of leukemias in mice, suggesting that characteristics of tumor suppressors may be common to these general coactivators p300 and CBP.[52]

In summary, we propose that activated Notch represses TGF-β-mediated signaling possibly through sequestration of coactivator p300, which contributes to the mechanisms of Notch-induced neoplastic transformation. Our current results indicate that Notch oncoproteins promote cell proliferation and tumor development partly by repressing the tumor suppressor Smad.

Acknowledgments

We thank K. Miyazono for p3TP-Lux, pcDNA3/TβRI(TD)-HA, pcDNA3/6Xmyc-Smad3 and pcDEF3/p300-Flag; J. L. Wrana for Flag-Smad2; R. Derynck for Flag-Smad3 and Flag-Smad4; T. Honjo for pEF-BOSneo-RBP-J (R218H); L. Strobl and U. Zimber-Strobl for pGa986-1. We are also grateful to C. Kato for her technical help. This work was supported in part by grants-in-aid (KAKENHI, numbers 13307029 and 14370300) and Special Coordination Funds for Promoting Science and Technology from the Ministry of Education, Culture, Sports, Science and Technology of Japan, and Health and Labor Sciences Research Grants (Research Grants on Pharmaceutical and Medical Safety) from the Ministry of Health, Labor and Welfare of Japan.

References

1 Artavanis-Tsakonas S, Rand MD, Lake R. Notch signaling: cell fate control and signal integration in development. *Science* 1999; **284**: 770–6.
2 Allman D, Punt JA, Izon DJ, Aster JC, Pear WS. An invitation to T and more: Notch signaling in lymphopoiesis. *Cell* 2002; **109**: S1–11.
3 Pui JC, Allman D, Xu L, DeRocco S, Karnell FG, Bakkour S, Lee JY, Kadesch T, Hardy RR, Aster JC, Pear WS. Notch1 expression in early lymphopoiesis influences B versus T lineage determination. *Immunity* 1999; **11**: 299–308.
4 Radtke F, Wilson A, Stark G, Bauer M, van Meerwijk J, MacDonald HR, Aguet M. Deficient T cell fate specification in mice with an induced inactivation of Notch1. *Immunity* 1999; **10**: 547–58.
5 Ellisen LW, Bird J, West DC, Soreng AL, Reynolds TC, Smith SD, Sklar J. TAN-1, the human homolog of the Drosophila notch gene, is broken by chromosomal translocations in T lymphoblastic neoplasms. *Cell* 1991; **66**: 649–61.
6 Robbins J, Blondel BJ, Gallahan D, Callahan R. Mouse mammary tumor gene int-3: a member of the notch gene family transforms mammary epithelial cells. *J Virol* 1992; **66**: 2594–9.
7 Aster JC, Pear WS, Hasserjian RP, Erba H, Davi F, Luo B, Scott M, Baltimore D, Sklar J. Functional analysis of the TAN-1 gene, a human homolog of Drosophila notch. *Cold Spring Harbor Symp Quant Biol* 1994; **59**: 125–36.
8 Pear WS, Aster JC, Scott ML, Hasserjian RP, Soffer B, Sklar J, Baltimore D. Exclusive development of T cell neoplasms in mice transplanted with bone marrow expressing activated Notch alleles. *J Exp Med* 1996; **183**: 2283–91.
9 Aster JC, Robertson ES, Hasserjian RP, Turner JR, Kieff E, Sklar J. Oncogenic forms of NOTCH1 lacking either the primary binding site for RBP-J or nuclear localization sequences retain the ability to associate with RBP-J and activate transcription. *J Biol Chem* 1997; **272**: 11 336–43.
10 Capobianco AJ, Zagouras P, Blaumueller CM, Artavanis-Tsakonas S, Bishop JM. Neoplastic transformation by truncated alleles of human NOTCH1/TAN1 and NOTCH2. *Mol Cell Biol* 1997; **17**: 6265–73.
11 Gallahan D, Callahan R. The mouse mammary tumor associated gene INT3 is a unique member of the NOTCH gene family (NOTCH4). *Oncogene* 1997; **14**: 1883–90.
12 Aster JC, Xu L, Karnell FG, Patriub V, Pui JC, Pear WS. Essential roles for ankyrin repeat and transactivation domains in induction of T-cell leukemia by Notch1. *Mol Cell Biol* 2000; **20**: 7505–15.
13 Bellavia D, Campese AF, Alesse E, Vacca A, Felli MP, Balestri A, Stoppacciaro A, Tiveron C, Tatangelo L, Giovarelli M, Gaetano C, Ruco L, Hoffman ES, Hayday AC, Lendahl U, Frati L, Gulino A, Screpanti I. Constitutive activation of NF-κB and T-cell leukemia/lymphoma in Notch3 transgenic mice. *EMBO J* 2000; **19**: 3337–48.
14 Dumont E, Fuchs KP, Bommer G, Christoph B, Kremmer E, Kempkes B. Neoplastic transformation by Notch is independent of transcriptional activation by RBP-J signalling. *Oncogene* 2000; **19**: 556–61.
15 Jeffries S, Capobianco AJ. Neoplastic transformation by Notch requires nuclear localization. *Mol Cell Biol* 2000; **20**: 3928–41.
16 Aster JC, Pear WS. Notch signaling in leukemia. *Curr Opin Hematol* 2001; **8**: 237–44.
17 Weng AP, Ferrando AA, Lee W, Morris JP, Silverman LB, Sanchez-Irizarry C, Blacklow SC, Look T, Aster JC. Activating mutations of *NOTCH1* in human T cell acute lymphoblastic leukemia. *Science* 2004; **306**: 269–71.
18 Weijzen S, Rizzo P, Braid M, Vaishnav R, Jonkheer SM, Zlobin A, Osborne BA, Gottipati S, Aster JC, Hahn WC, Rudolf M, Siziopikou K, Kast WM, Miele L. Activation of Notch-1 signaling maintains the neoplastic phenotype in human Ras-transformed cells. *Nat Med* 2002; **8**: 979–86.
19 Yan XQ, Sarmiento U, Sun Y, Huang G, Guo J, Van Juan TG, Qi MY, Scully S, Senaldi G, Fletcher FA. A novel Notch ligand, Dll4, induces T-cell leukemia/lymphoma when overexpressed in mice by retroviral-mediated gene transfer. *Blood* 2001; **98**: 3793–9.
20 Zagouras P, Stifani S, Blaumueller CM, Carcangiu ML, Artavanis-Tsakonas S. Alterations in Notch signaling in neoplastic lesions of the human cervix. *Proc Natl Acad Sci USA* 1995; **92**: 6414–18.
21 Jundt F, Anagnostopoulos I, Forster R, Mathas S, Stein H, Dorken B. Activated Notch1 signaling promotes tumor cell proliferation and survival in Hodgkin and anaplastic large cell lymphoma. *Blood* 2002; **99**: 3398–403.
22 Oswald F, Täuber B, Dobner T, Bourteele S, Kostezka U, Adler G, Liptay S, Schmid RM. p300 acts as a transcriptional coactivator for mammalian Notch-1. *Mol Cell Biol* 2001; **21**: 7761–74.
23 Nishihara A, Hanai J-I, Okamoto N, Yanagisawa J, Kato S, Miyazono K, Kawabata M. Role of p300, a transcriptional coactivator, in signalling of TGF-β. *Genes Cells* 1998; **3**: 613–23.
24 Pouponnot C, Jayaraman L, Massague J. Physical and functional interaction of Smads and p300/CBP. *J Biol Chem* 1998; **273**: 22 865–8.
25 Massague J, Blain SW, Lo RS. TGF-β signaling in growth control, cancer, and heritable disorders. *Cell* 2000; **103**: 295–309.
26 Derynck R, Akhurst RJ, Balmain A. TGF-β signaling in tumor suppression and cancer progression. *Nat Genet* 2001; **29**: 117–29.
27 Wakefield LM, Roberts AB. TGF-β signaling. positive and negative effects on tumorigenesis. *Curr Opin Genet Dev* 2002; **12**: 22–9.
28 Heldin CH, Miyazono K, ten Dijke P. TGF-β signalling from cell membrane to nucleus through SMAD proteins. *Nature* 1997; **390**: 465–71.
29 Chang H, Brown CW, Matzuk MM. Genetic analysis of the mammalian transforming growth factor-β superfamily. *Endo Rev* 2002; **23**: 787–823.
30 Nakao A, Imamura T, Souchelnytskyi S, Kawabata M, Ishisaki A, Oeda E, Tamaki K, Hanai J, Heldin CH, Miyazono K, ten Dijke P. TGF-β receptor-mediated signaling through Smad2, Smad3 and Smad4. *EMBO J* 1997; **16**: 5353–62.
31 Massague J. How cells read TGF-β signals. *Nat Rev Mol Cell Biol* 2000; **1**: 169–78.
32 Massague J, Chen YG. Controlling TGF-β signaling. *Genes Dev* 2000; **14**: 627–44.
33 Kurokawa M, Mitani K, Irie K, Matsuyama T, Takahashi T, Chiba S, Yazaki Y, Matsumoto K, Hirai H. The oncoprotein Evi-1 represses TGF-β signalling by inhibiting Smad3. *Nature* 1998; **394**: 92–6.
34 Imai Y, Kurokawa M, Izutsu K, Hangaishi A, Maki K, Ogawa S, Chiba S, Mitani K, Hirai H. Mutations of Smad4 gene in acute myelogeneous leukemia and their functional implications in leukemogenesis. *Oncogene* 2001; **20**: 88–96.
35 Kumano K, Chiba S, Shimizu K, Yamagata T, Hosoya N, Saito T, Takahashi T, Hamada Y, Hirai H. Notch1 inhibits differentiation of hematopoietic cells by sustaining GATA-2 expression. *Blood* 2001; **98**: 3283–9.
36 Shimizu K, Chiba S, Saito T, Kumano K, Hamada Y, Hirai H. Functional diversity among Notch1, Notch2, and Notch3 receptors. *Biochem Biophys Res Commun* 2002; **291**: 775–9.
37 Nofziger D, Miyamoto A, Lyons KM, Weinmaster G. Notch signaling imposes two distinct blocks in the differentiation of C2C12 myoblasts. *Development* 1999; **126**: 1689–702.
38 Liu D, Black BL, Derynck R. TGF-β inhibits muscle differentiation through functional repression of myogenic transcription factors by Smad3. *Genes Dev* 2001; **15**: 2950–66.
39 Shimizu K, Chiba S, Hosoya N, Kumano K, Saito T, Kurokawa M, Kanda Y, Hamada Y, Hirai H. Binding of Delta1, Jagged1, and Jagged2 to Notch2 rapidly induces cleavage, nuclear translocation, and hyperphosphorylation of Notch2. *Mol Cell Biol* 2000; **20**: 6913–22.
40 Chung CN, Hamaguchi Y, Honjo T, Kawaichi M. Site-directed mutagenesis study on DNA binding regions of the mouse homologue of Suppressor of Hairless, RBP-Jκ. *Nucl Acids Res* 1994; **22**: 2938–44.
41 Rao P, Kadesch T. The intracellular form of notch blocks transforming growth factor β-mediated growth arrest in Mv1Lu epithelial cells. *Mol Cell Biol* 2003; **23**: 6694–701.

42 Takizawa T, Ochiai W, Nakashima K, Taga T. Enhanced gene activation by Notch and BMP signaling cross-talk. *Nucl Acids Res* 2003; **31**: 5723–31.
43 Itoh F, Itoh S, Goumans MJ, Valdimarsdottir G, Iso T, Dotto GP, Hamamori Y, Kedes L, Kato M, ten Dijke P. Synergy and antagonism between Notch and BMP receptor signaling pathways in endothelial cells. *EMBO J* 2004; **23**: 541–51.
44 Blokzijl A, Dahlqvist C, Reissmann E, Falk A, Moliner A, Lendahl U, Ibanez CF. Cross-talk between the Notch and TGF-β signaling pathways mediated by interaction of the Notch intracellular domain with Smad3. *J Cell Biol* 2003; **163**: 723–8.
45 Zavadil J, Cermak L, Soto-Nieves N, Bottinger EP. Integration of TGF-β/Smad and Jagged1/Notch signalling in epithelial-to-mesenchymal transition. *EMBO J* 2004; **23**: 1155–65.
46 Kamei Y, Xu L, Heinzel T, Torchia J, Kurokawa R, Gloss B, Lin SC, Heyman RA, Rose DW, Glass CK, Rosenfeld MG. A CBP integrator complex mediates transcriptional activation and AP-1 inhibition by nuclear receptors. *Cell* 1996; **85**: 403–14.
47 Lee CW, Sorensen TS, Shikama N, La Thang NB. Functional interplay between p53 and E2F through co-activator p300. *Oncogene* 1998; **16**: 2695–710.
48 Webster GA, Perkins ND. Transcriptional cross talk between NF-κB and p53. *Mol Cell Biol* 1999; **19**: 3485–95.
49 Sheppard KA, Phelps KM, Williams AJ, Thanos D, Glass CK, Rosenfeld MG, Gerritsen ME, Collins T. Nuclear integration of glucocorticoid receptor and nuclear factor-κB signaling by CREB-binding protein and steroid receptor coactivator-1. *J Biol Chem* 1998; **273**: 29 291–4.
50 Horvai AE, Xu L, Korzus E, Brard G, Kalafus D, Mullen TM, Rose DW, Rosenfeld MG, Glass CK. Nuclear integration of JAK/STAT and Ras/AP-1 signaling by CBP and p300. *Proc Natl Acad Sci USA* 1997; **94**: 1074–9.
51 Lubman OY, Korolev SV, Kopan R. Anchoring notch genetics and biochemistry: structural analysis of the ankyrin domain sheds light on existing data. *Mol Cell* 2004; **13**: 619–26.
52 Goodman RH, Smolik S. CBP/p300 in cell growth, transformation, and development. *Genes Dev* 2000; **14**: 1553–77.
53 Kopan R, Ilagan MX. γ-Secretase: proteasome of the membrane? *Nature Rev Mol Cell Biol* 2004; **5**: 499–504.
54 Shawber C, Nofziger D, Hsieh JJ-D, Lindsell C, Bogler O, Hayward D, Weinmaster G. Notch signaling inhibits muscle cell differentiation through a CBF1-independent pathway. *Development* 1996; **122**: 3765–73.
55 Muraoka M, Konishi M, Kikuchi-Yanoshita R, Tanaka K, Shitara N, Chong JM, Iwama T, Miyaki M. p300 gene alterations in colorectal and gastric carcinomas. *Oncogene* 1996; **12**: 1565–9.
56 Gayther SA, Batley SJ, Linger L, Bannister A, Thorpe K, Chin SF, Daigo Y, Russell P, Wilson A, Sowter HM, Delhanty JDA, Ponder BAJ, Kouzarides T, Caldas C. Mutations truncating the EP300 acetylase in human cancers. *Nat Genet* 2000; **24**: 300–3.
57 Suganuma T, Kawabata M, Ohshima T, Ikeda M. Growth suppression of human carcinoma cells by reintroduction of the p300 coactivator. *Proc Natl Acad Sci USA* 2002; **99**: 13 073–8.

 doi: 10.1111/j.1349-7006.2005.00048.x

ELSEVIER

EXPERIMENTAL HEMATOLOGY

Experimental Hematology 33 (2005) 1459–1469

Hematopoietic stem cells expanded by fibroblast growth factor-1 are excellent targets for retrovirus-mediated gene delivery

Aleksandra Crcareva[a,b,d], Toshiki Saito[a], Atsushi Kunisato[a,b,e], Keiki Kumano[a,b], Takahiro Suzuki[a,c], Mamiko Sakata-Yanagimoto[a,b], Masahito Kawazu[a], Aleksandar Stojanovic[d], Mineo Kurokawa[a], Seishi Ogawa[a,c], Hisamaru Hirai[a,b], and Shigeru Chiba[a,b]

[a]*Departments of Hematology/Oncology;* [b]*Cell Therapy/Transplantation Medicine, and* [c]*Regeneration Medicine for Hematopoiesis, University of Tokyo, Tokyo, Japan;* [d]*Department of Hematology, Clinical Center, Skopje, Macedonia; and* [e]*Kirin Brewery Co., LTD Pharmaceutical Research Laboratories, Takasaki, Japan*

(Received 6 May 2005; revised 31 August 2005; accepted 1 September 2005)

Objective. **For the study of the function of genes of interest in hematopoietic stem cells (HSCs) and for successful gene therapy, it is fundamental to develop a method of efficient gene transfer into HSCs. In mice experiments, efforts have been made to raise the transduction efficiency by modifying the vectors, administrating 5-fluorouracil (5-FU) to donor mice, selecting cytokine cocktails to better sustain the long-term repopulating potential of the stem cells, and so on. The objective of this study is to examine whether the use of fibroblast growth factor-1 (FGF-1)-expanded bone marrow cells provide an improved source for retroviral gene delivery to HSCs.**

Materials and Methods. **Unfractionated bone marrow cells from one mouse were cultured in serum-free medium containing FGF-1. Both floating and attached cells were transferred to retronectin precoated dishes and infected with virus supernatant from MP34 cells stably transduced with pMY/GFP retrovirus. After 3-day infection, the green fluorescence protein–positive fraction was sorted and the cells were transplanted to lethally irradiated mice.**

Results. **The experiments illustrated that the number of bone marrow–derived competitive repopulation units (CRUs) was increased from 600 to 9300 per mouse after a 3-week culture period with FGF-1. Following retroviral transduction of the expanded cells, the absolute number of sorted retrovirus-transduced CRUs was 4200. Using these retrovirus-transduced cells in noncompetitive reconstitution assay, we achieved radiation protection and long-term bone marrow reconstitution in 100% of the recipients with average myeloid and lymphoid chimerisms of 70% and 50%, respectively, even if we transplanted 150 recipients with cells derived from a single donor mouse.**

Conclusion. **In conclusion, FGF-1-expanded bone marrow cells constitute an excellent source of stem cells that could be used in a range of gene delivery protocols.** © **2005 International Society for Experimental Hematology. Published by Elsevier Inc.**

Hematopoietic stem cells (HSCs) are clonogenic cells with capacity to self-renew and differentiate into progenitor cells and mature blood cells of all hematopoietic lineages. Gene delivery to HSCs is key to the study of genes of interest in HSCs and their various progenies for experimental purposes, as well as for gene therapy of hematopoietic and immune disorders. In most of the experimental protocols for HSC-targeted gene delivery, retrovirus-mediated gene transfer methods have been used. The difficulty is that cell division is requisite for the retrovirus to be introduced into the cells and HSCs are quiescent in nature. The use of lentiviral vectors is more efficient as they do not require cell division for gene transduction, but it requires higher biosafety levels.

Offprint requests to: Shigeru Chiba, M.D., Ph.D., Department of Cell Therapy and Transplantation Medicine, University of Tokyo Hospital, 7-3-1 Hongo, Bunkyo-ku, Tokyo 113-8655, Japan; E-mail: schiba-tky@umin.ac.jp

The present address for Aleksandra Crcareva is Department of Stem Cell Biology, University of Groningen; the present address for Toshiki Saito is Transplantation Biology Research Center, BMT Section, MGH-East, Boston, Massachusetts, USA.

0301-472X/05 $–see front matter.
doi: 10.1016/j.exphem.2005.09.001

It has been a major challenge for the development of HSC culture procedures to allow transplantable stem cells to proliferate without loss of their stem cell activity. Modifications of cytokine combinations used for HSC expansion [1–3] have resulted only in modest improvements in gene transfer into HSCs because any cytokine combination induces some degree of differentiation in the HSCs concomitant with their cell division. As an alternative gene transfer strategy, administration of 5-fluorouracil (5-FU) to donor mice has been used to enrich the HSCs. 5-FU is selectively cytotoxic for cycling cells while forcing quiescent HSCs to go into cycle. It is known that 5-FU administration enhances gene transfer into HSCs up to 10-fold [4] but there is also evidence that treatment with 5-FU reduces the engraftment potential of bone marrow (BM) cells [5].

Recently, a cogent method for in vitro expansion of mouse long-term repopulating cells using fibroblast growth factor-1 (FGF-1) as a single exogenous growth factor was described [6]. We confirmed that this method is highly reproducible and that the growing cells after 3 weeks of this culture contain an abundant number of long-term and multilineage repopulating cells. Thus, we expected that these cells would serve as an excellent source for retrovirus-mediated gene delivery.

Interestingly, limiting dilution experiments revealed that there was a 15.3-fold increase in the number of competitive repopulation units (CRUs) cultured with FGF-1 and that 45% of the expanded CRUs could be recovered by sorting as retrovirus-transduced cells.

Materials and methods

Mice

C57BL/6 (B6-Ly5.2) mice were purchased from Narc (Tokyo, Japan). Mice congenic for Ly5 locus (B6-Ly5.1), gifts from H. Nakauchi (Institute of Medical Science, University of Tokyo, Tokyo, Japan), were bred and maintained at Sankyo Labo Service (Tsukuba, Japan). Ly5.1/5.2 mice were obtained from mating pairs of B6-Ly5.1 males and B6-Ly5.2 females and were maintained in the animal facility of the University of Tokyo. Eight- to 10-week old mice were used as recipients. Mice were treated based on the University of Tokyo Animal Experiment Manual.

Cytokines

The Flt3 ligand (FL) was purchased from Genzyme (Boston, MA, USA), and the other cytokines used were generated in Kirin Brewery Research Laboratory (Takasaki, Japan).

Establishment of virus producing stable cell lines

GP-293 packaging cells (Clontech, Palo Alto, CA, USA) were transiently transfected with vesicular stomatitis virus glycoprotein (pVSV-G; Clontech) and pMY/IRES-EGFP [7] (a gift from T. Kitamura, IMSUT, Tokyo, Japan). After 48 hours, virus supernatant was collected and used to infect ψMP34 cells [8] (a gift from Wakunaga Pharmaceuticals, Hiroshima, Japan), which carries an envelope protein from Molony murine leukemia virus [9,10].

ψMP34 cells expressing green fluorescence protein (GFP) at high levels were clone-sorted with FACS Vantage (Becton Dickinson, Franklin Lakes, NJ, USA) and the clones producing individual viruses at the highest titers were selected.

Virus-producing ψMP34 cells were cultured in 3 mL Dulbecco's modified essential medium (Invitrogen, Grand Island, NY, USA) supplemented with 10% fetal calf serum and penicillin streptokinase in collagen type I–coated plates (Corning Inc., Corning, NY, USA). After 48 hours, when 90% confluence was reached, the culture medium was collected and filtrated through 0.45-μm filters (Pall Corporation, Ann Harbor, MI, USA). Virus was concentrated by centrifugation at 18,000*g* for 4 hours at 4°C. The titer of the concentrated virus was defined by transduction of NIH3T3 cells and analysis of GFP expression with FACS Calibur (Becton Dickinson). All the concentrated viral supernatants showed efficiencies of 3.5 to 4 × 10^8 NIH3T3 cell infection per milliliter.

Stem cell expansion

BM cells were cultured with FGF-1 and heparin as previously described [6]. Briefly, unfractionated BM cells with neither erythrocyte lysis nor gradient centrifugation from a 10- to 12-week-old B6-Ly5.1 mouse were cultured for 3 weeks in 5 mL StemSpan serum-free medium (StemCell Technologies, Vancouver, BC, Canada) in the presence of 10 ng/mL FGF-1 (Invitrogen) and 10 μg/mL heparin (Sigma, St. Louis, MO, USA) in a six-well noncoated plate. The density of the cells was 5 × 10^6 cells/well. Two plates (12 wells) were used to culture BM cells obtained from a single mouse. Twice a week, the medium was changed by removing half the media from the well and gently adding equal amount of the same fresh media without resuspending the cells.

Stem cell enrichment

BM mononuclear cells were obtained from 10- to 12-week-old mice and lineage marker–negative, c-Kit^+ and $Sca1^+$ (KSL) cells were sorted with FACS Vantage as previously described [11,12].

Retrovirus gene transfer

A schematic diagram of the transduction protocol of the FGF-1-expanded cells is given in Figure 1B. Six wells from a 24-well noncoated plate were covered with 500 μL of 25 μg/mL RetroNectin (Takara, Shiga, Japan) and incubated overnight at 4°C or 2 hours at room temperature. The wells were then washed with phosphate-buffered saline (PBS) and covered with 2% bovine serum albumin for 30 minutes at room temperature. After being washed with PBS again, 500 μL of the unconcentrated virus-containing medium was put in the wells and incubated at 37°C for 4 hours. Next, the supernatant was discarded and the wells were gently washed with PBS.

After centrifugation of virus-containing medium, the supernatants were removed and the pellets were resuspended in 300 μL of StemSpan medium containing one of the following three cytokine cocktails: 10 ng/mL FGF-1+100 ng/mL stem cell factor (SCF)+100 ng/mL TPO, 100 ng/mL SCF + 100 ng/mL TPO, or 10 ng/mL FGF-1 alone. Then, these concentrated viruses were mixed with a 200-μL suspension of 3.5 × 10^5 cultured cells resuspended in 300 μl of the same cytokine cocktails described above (multiplicity of infection [MOI], 300–340; see below for details).

Subsequently, the 3-week cultured BM cells were collected from one well. The floating and adherent cells were collected by

pipetting and 0.1% trypsin treatment, respectively. Then the cells were washed with PBS to remove the heparin and resuspended in 200 μL of StemSpan medium containing one of the cytokine cocktails that was used to prepare the concentrated viruses. These cell suspensions were then mixed with the concentrated viruses and overlaid on retronectin-coated wells (see above; 500 μL total volume/well of medium containing same cytokine cocktail). The cells were incubated at 37°C in 5% CO_2 for 3 days. Concentrated viruses (150 μL) were daily refurnished after the same volume of infection medium had been discarded. At the end of the 72-hour transduction, the floating and adherent cells were collected and GFP-positive cells were sorted and used for competitive and noncompetitive repopulation assays.

Retroviral transduction of the KSL cells was performed as previously described [12]. Briefly, 5×10^4 KSL cells were collected from 10 to 12 mice and seeded at a concentration of 1×10^4 in one retronectin-coated well of a 24-well dish and cultured in StemPro34 medium (Invitrogen) containing 50 ng/mL SCF, 20 ng/mL TPO, and 20 ng/mL FL in addition to the concentrated virus prepared in the same medium (MOI, 1.1–1.2 $\times$ 10^4). Twenty-four hours after the culture, half of the medium was replaced with fresh concentrated virus and cultured for another 24 hours. After 48 hours the GFP-positive cells were sorted.

Noncompetitive repopulation assays

After sorting the GFP-positive cells from the FGF-1-expanded virus-transduced cells and from the virus-transduced KSL cells, we injected 1×10^5 and 1×10^3 cells, respectively, into a tail vein of 9.5 Gy irradiated B6-Ly5.2 recipient mice. Peripheral blood count and percentage of GFP-positive cells were evaluated every 2 weeks with FACS Calibur. Twelve weeks after the primary transplantation, the mice transplanted with FGF-1-expanded and virus-transduced cells were sacrificed, the GFP-positive cells from the BM were sorted, and 1×10^5 cells were injected into the B6-Ly5.2 secondary recipient after 9.5-Gy irradiation.

Competitive repopulating unit analysis

The experiment was performed on three cohorts of mice. In the first cohort, 2×10^5, 2×10^4, or 5×10^3 unfractionated fresh BM cells; in the second cohort, 1×10^5, 1×10^4, 3×10^3, 1×10^3, 3×10^2 3-week cultured cells in the presence of FGF-1; and in the third cohort, 1×10^5, 1×10^4 3×10^3, 1×10^3, 3×10^2 3-week cultured and then sorted retrovirus-transduced cells, respectively (individually designated as test cells) from B6-Ly5.1 mice were transplanted together with 2×10^5 competitor cells from Ly5.1/5.2 mice to 9.5 Gy irradiated B6-Ly5.2 recipients. Five to eight recipients were used in each arm. Ten weeks after transplantation, the proportion of the individual donor cells in the peripheral blood was determined using specific antibodies (see below). The animals were considered to be positive if >2% of both myeloid and lymphoid (B+T) cells were of donor origin 10 weeks after transplant. The frequency of the CRUs in the test cells was analyzed by Poisson statistics and the statistical software L-Calc (StemCell Technologies).

Flow cytometry

Flow cytometric analyses were performed on a FACS Calibur. The following antibodies were used: fluorescein isothiocyanate-CD45.2, phycoerythrin (PE)-Sca-1, PE-B220, PE-CD3, PE-CD45.1, allophycocyanate (APC)-c-kit, APC-CD4, APC-CD8, APC-CD45.2, peridinin chlorophyll protein (PerCp)-B220, PerCP-Cy5.5-CD45.2, and biotinylated CD45.1 and CD45.2. All antibodies were purchased from BD PharMingen (San Diego, CA, USA). The samples for staining were prepared by standard protocols. GFP fluorescence was detected using detector channel FL-1.

Results

Characterization of the BM cells cultured with FGF-1

We cultured unfractionated BM cells from B6-Ly5.1 mouse in heparin-supplemented serum-free medium in the presence of FGF-1 as a single cytokine, as described previously [6]. Cell numbers declined in the early phase of the culture, but after 2 weeks slowly started to increase. Most of the cells in the well at this time were nonadherent. As soon as small blast-like colonies loosely attached to the bottom appeared, the cells began expanding rapidly. We found that the percentage of Sca-1^+c-Kit^+ (KS) fraction gradually increased (0.13% and 11% after 1 and 2 weeks, respectively; data not shown) and reached the maximum of ~30% 3 weeks after culture initiation. In contrast, in BM cells cultured in the same medium but without FGF-1 and heparin, almost no KS cells were detected 3 weeks after the culture (Fig. 1A). We confirmed that 1×10^5 of unfractionated cells that had been grown in the presence of FGF-1 for 3 weeks conferred radiation resistance in the absence of rescue cells, and multilineage blood chimerism (>80% in myeloid and >50% in lymphoid populations) was observed in lethally irradiated congenic recipient mice at 3 months posttransplant (data not shown).

We also cultured unfractionated BM cells for 3 weeks in the same medium but in the presence of different cytokines or cytokine combinations such as 100 ng/mL SCF alone, 100 ng/mL SCF + 30 ng/mL TPO, or 100 ng/mL SCF + 30 ng/mL FGF-1. Interestingly, despite the fact that we detected similar ratios of KS cells in all of the above conditions, the percents of the donor-derived cell in the lethally irradiated recipients 3 months posttransplant in noncompetitive repopulation assays were about 10% and 5% in the myeloid and lymphoid populations, respectively (data not shown). Thus we concluded that only the cells cultured with FGF-1 alone potentially contain expanded HSCs that could be a target for retrovirus-mediated gene delivery.

Successful transduction of the FGF-1 expanded BM cells and characterization of the transduced cells

When we subjected FGF-1-cultured BM cells to the retrovirus transduction protocol in the presence of FGF-1 alone, the cells adhered to the bottom of the plate and slightly increased in number. Appearance of GFP-positive cells was very rare until 72 hours after transduction (data not shown). In contrast, in the presence of FGF-1 + SCF + TPO or SCF + TPO, most of the cells adhered to the bottom of the plate within 4 hours, and floating cells began to emerge on the

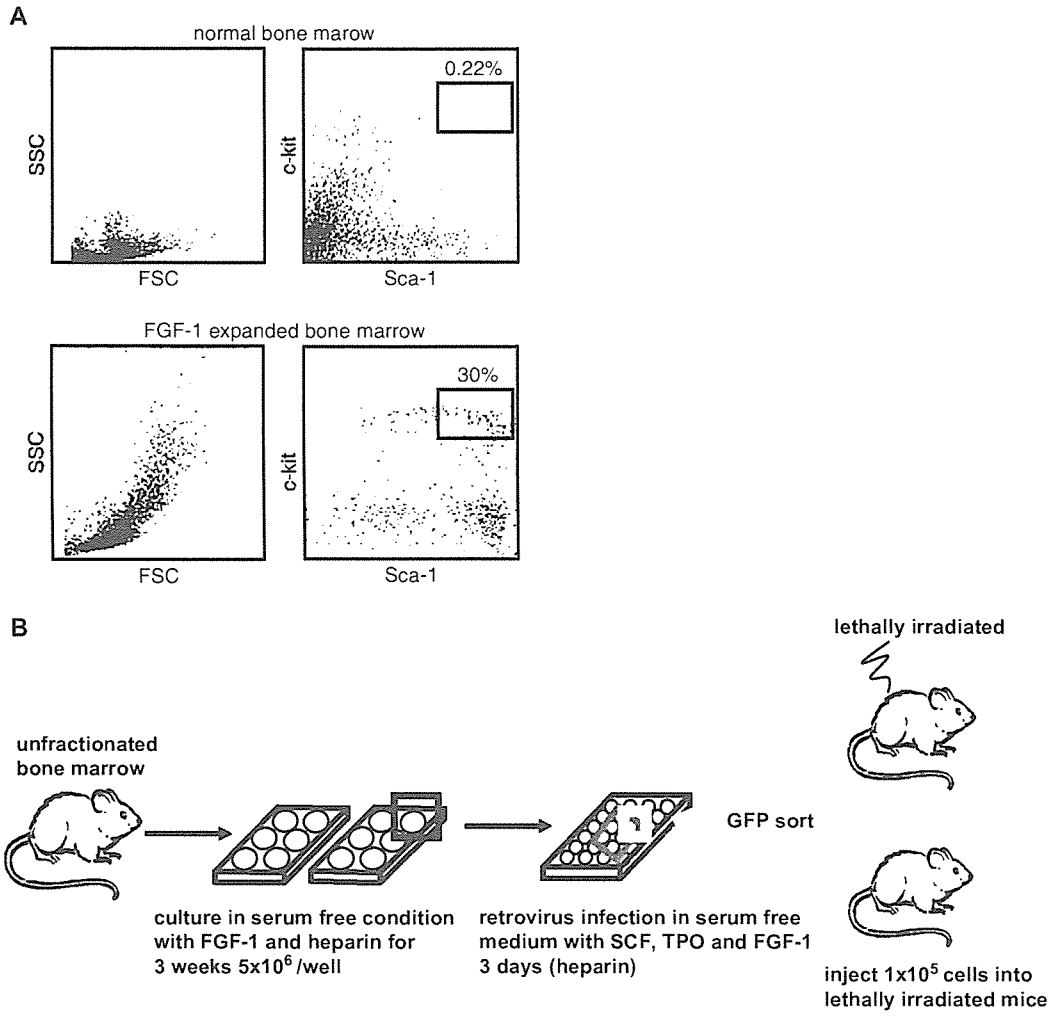

Figure 1. Characterization of BM cells cultured with FGF-1 and schematic representation of the method. **(A):** Unfractionated BM cells were cultured in the presence of FGF-1 and heparin. The cells cultured for 3 weeks showed highest percentage of $Sca1^+c\text{-}kit^+$ fraction (30%) and were used for the subsequent experiments. Cells cultured in the same conditions but without FGF-1 gave rise to almost no $Sca1^+c\text{-}kit^+$ cells. **(B):** Schematic representation of the experimental design. Unfractionated BM cells from a single mouse were cultured in two 6-well plates at a cell density of 5×10^6/well for a 3-week period with FGF-1 and heparin in serum-free medium. Both adherent and floating cells from one of these wells were then transferred to six wells of a 24-well plate and the transduction was performed as described in the Methods section. An average of 2×10^5 GFP-positive cells from each of these wells was sorted and injected into two lethally irradiated mice. For each recipient mouse, we used 1/150 of the cells from a single donor. Engraftment was achieved in 100% recipients.

next day and they then rapidly increased in number. Under the microscope, the majority of both floating and adherent cells were GFP-positive after 72 hours (Fig. 2A and data not shown).

By flow cytometric analyses, we confirmed much higher transduction efficiency when using the combinations of FGF-1 + SCF + TPO and SCF + TPO than FGF-1 alone during the transduction procedure (Fig. 2B). We observed that comparable ratios of $Sca1^+$ and $Sca1^-$ cells, and $c\text{-}Kit^+$ and $c\text{-}Kit^-$ cells were transduced with the combinations of FGF-1 + SCF + TPO and SCF + TPO (Fig. 2B). The percentage and absolute number of retrovirus-transduced KS cells were also greater when combinations of FGF-1 + SCF + TPO or SCF + TPO were chosen. Mudifewer KS cells were transduced in the presence of FGF-1 alone (Fig. 2B). The transduction efficiency was similar between the combinations of FGF-1 + SCF + TPO and SCF + TPO. The percentage of remaining KS cells, however, was slightly but consistently greater with the combination of FGF-1 + SCF + TPO (11 ± 1%) than with the combination of SCF + TPO (8 ± 0.8%; Fig. 2B). Thus, we decided to choose the former combination for our subsequent experiments. We sorted all the GFP-positive cells after a 3-week culture with FGF-1 alone and 3-day transduction with SCF + TPO + FGF-1. Interestingly, most of the GFP-positive cells in this condition were

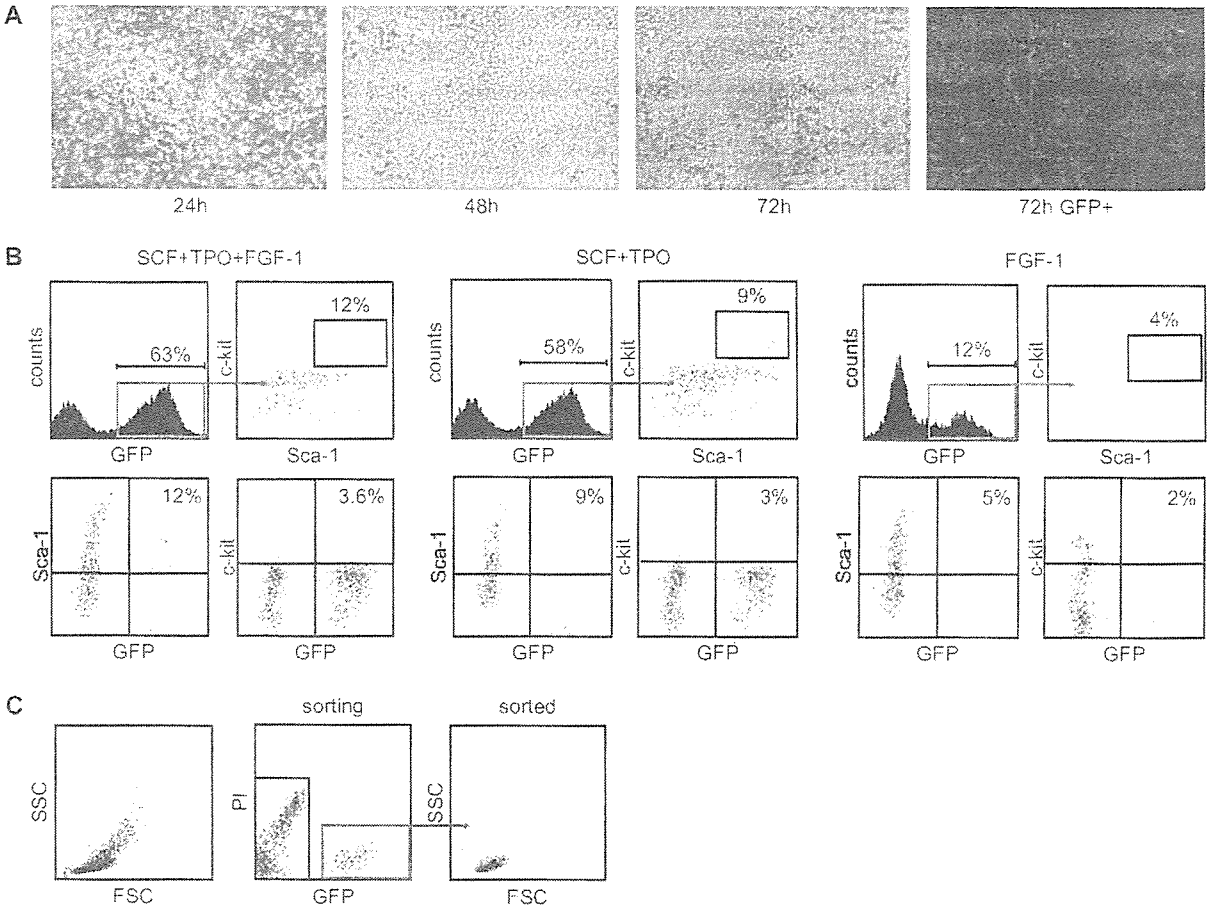

Figure 2. Successful transduction of the FGF-1-expanded BM cells. **(A):** Microscopic image of the cells during transduction procedure. Twenty-four hours after the transduction, almost all the cells attached to the bottom (left panel). The floating cells increased in number over the next 48 hours (second panel) and overgrew the adherent cells 72 hours (third panel) after commencing the transduction. Fluorescent microscopic observation showing GFP expression (right panel) is shown. Original magnification, ×40. **(B):** Optimization of the transduction protocol. After 3-week culture with FGF-1 and heparin, both adherent and nonadherent cells were transferred to fibronectin-coated dishes with medium containing the cytokines as previously described. These were subsequently transduced with virus supernatant from ψMP34 cells stably transduced with pMY/mock-IIG retrovirus. Best results were obtained when using the combination of FGF-1, SCF, and TPO. **(C):** All GFP-positive cells were sorted after a 3-day transduction. Characterization of the sorted cells is shown. Most of the GFP-positive cells are confined to the lymphocyte gate.

confined to the lymphocyte gate (Fig. 2C). These cells were used for repopulation experiments.

Attempts to use cells cultured with FGF-1 for longer than 3 weeks and to shorten or prolong the transduction period resulted in reduction of the percentage of GFP-positive cells (data not shown).

Competitive reconstitution experiments

In order to compare the absolute numbers of HSCs in fresh BM before culture, in the population after culture but before transduction, and in the retrovirus-transduced cell population, we performed limiting dilution and competitive repopulation experiments. Serially reduced numbers of cells from the three sources were transplanted into lethally irradiated recipients, together with 2×10^5 competitor BM cells. At 4, 8, and 10 weeks posttransplant, peripheral blood cells were analyzed to examine the level of donor-derived test cells. The CRU frequencies in unfractionated fresh BM cells, FGF-1-cultured cells, and cultured and then sorted retrovirus-transduced cells were 1/82,000 (with 95% confidence interval 1/34,765–193,475), 1/2700 (1/1399–5211) and 1/3600 (1/1840–7021), respectively (Fig. 3B). Because the starting cell numbers per donor mouse were about 5×10^7 fresh BM cells, $2.5 \pm 0.41 \times 10^7$ FGF-1-cultured cells, and $1.5 \pm 0.41 \times 10^7$ cultured and sorted retrovirus-transduced cells, the absolute numbers of CRUs in each population were calculated to be about 600, 9300 and 4200, respectively. Ultimately, we can conclude that the markedly higher number of retrovirus-transduced HSCs is available in the FGF-1-expanded population

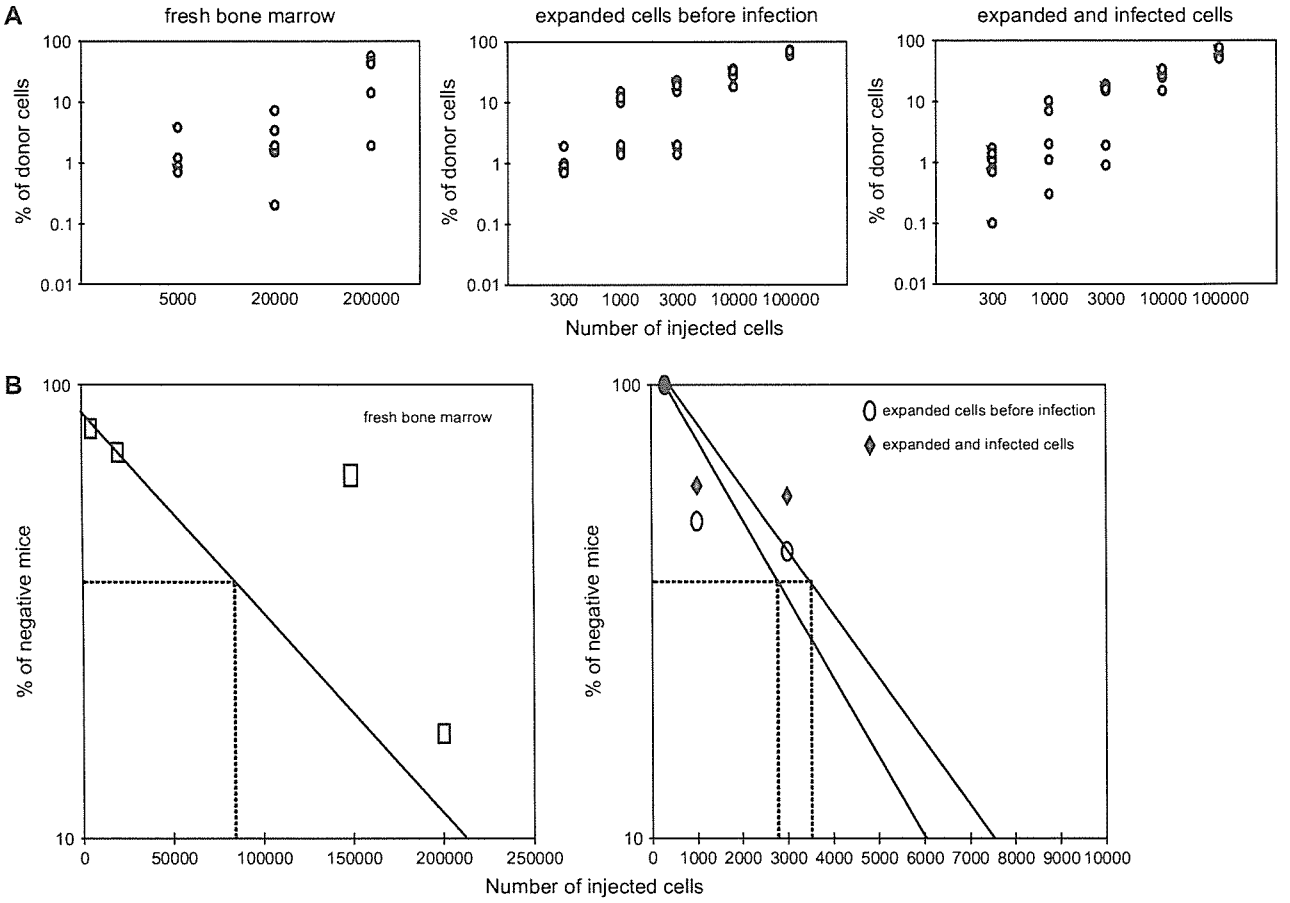

Figure 3. **(A)** Competitive repopulating unit measurements in fresh, FGF-1-expanded and FGF-1-expanded and transduced BM cells. The percentage of donor-derived cells in each cohort of mice is presented. A mouse was considered to be positive if >2% of test cells were detected in both myeloid and lymphoid lineages in the peripheral blood of the recipients 10 weeks after transplant. **(B):** Relation between the test cell dose and the number of engrafted mice was analyzed by Poisson statistics and the CRU frequency is presented.

compared to those in the fresh BM, which should be only a fraction of 600 per mouse.

Contribution of the GFP-positive cells in the recipient mice

To characterize the FGF-1-expanded and retrovirus-transduced HSCs, we transplanted 1×10^5 GFP-positive cells per recipient without competitors. Based on the competitive repopulation assay, this number of retrovirus-transduced cells was expected to provide long-term engraftment. Because the average number of GFP-positive cells that was sorted was about 1.5×10^7 (per experiment initiated from BM cells derived from a single donor mouse), BM cells from a single mouse could be engrafted to 150 recipient mice (Table 1). In the recipient mice, contribution of GFP-positive cells in the myeloid cells was 79 ± 6% at 4 weeks posttransplant. The chimerism was slightly reduced to 67 ± 4.4% but sustained at these levels for 12 weeks. The chimerism of GFP-positive cells in the lymphoid compartment was 43 ± 5% at 4 weeks and slowly increased to 50 ± 6.3% until 12 weeks posttransplant (Fig. 4A and Table 1). We performed transplantation into five to eight recipient mice each in six independent experiments (more than 50 in total), with very consistent results.

Typically, HSCs used for gene delivery are fresh BM cells obtained from 5-FU-treated mice or fresh lineage-negative cells prepared from BM of untreated mice [12–16]. In order to directly compare our protocol with other methods, we transduced freshly purified KSL cells from normal mice with the retrovirus that was used in the transduction of FGF-1-cultured cells. In the transduction procedure, we used a cytokine combination of SCF, TPO, and Flt3 ligand because we had previously evaluated that this combination gave the best results in retrovirus-transduced cell transplantations. After sorting, we transplanted 1×10^3 GFP-positive cells into irradiated recipients. This procedure conferred respective peripheral blood chimerism of 15 ± 5.2% and 7.2 ± 6.1% in the myeloid and lymphoid lineages at 4 weeks posttransplant. However, the chimerism at 12 weeks posttransplant was always

Table 1. Comparison between freshly obtained KSL cells and FGF-1-treated bone marrow as a target for retrovirus-mediated gene delivery

Source	Fresh KSL cells	FGF-1-treated bone marrow
Number of donor mice	10–12	1
Number of available cells before transduction	$5.0 \pm 3.4 \times 10^4$	$2.5 \pm 0.41 \times 10^7$
Number of cells after transduction	$5.0 \pm 2.1 \times 10^4$	$5.2 \pm 0.52 \times 10^7$
Percentage of GFP-positive cells (%)	51 ± 4.1	57 ± 7.7
Number of cells after sorting	$6 \pm 1.2 \times 10^3$	$1.5 \pm 0.41 \times 10^7$
Number of cells injected into one recipient to achieve short-term chimerism w/o competitors	1×10^3	1×10^5
Percentage of donor chimerism at 12 weeks posttransplant		
Myeloid (%)	0.8 ± 0.6	67 ± 4.4
Lymphoid (%)	1.2 ± 1.5	50 ± 6.3
Number of recipient mice	~6	~150

The data is calculated as mean value ± SD from six independent experiments (13 animals for KSL cells and 46 animals for FGF-1-treated bone marrow cells). A parallel comparison of the two sources is given. When using KSL cells the number of mice required to collect only 5×10^4 cells was 10 to 12. This is in contrast to the FGF-1-treated bone marrow cells when just one mouse was used. Still, the number of recipient mice was ~6 and ~150, when using KSL or FGF-1-treated cells, respectively. Furthermore, the later ones provided higher number of GFP-positive cells and higher donor chimerism in the peripheral blood of the recipients 12 weeks after transplant than the previous. KSL, $Lin^-c\text{-}Kit^+Scal^+$ cells; FGF-1, fibroblast growth factor-1; GFP, green fluorescence protein.

<2% in both lineages. The comparison between the FGF-1-cultured cells and freshly obtained KSL cells is summarized in Fig. 4A and Table 1.

The multilineage reconstitution in the peripheral blood of the mice injected with FGF-1-expanded and transduced cells is presented in Figure 4B. Figure 4C demonstrates the contribution of these cells in hematopoietic organs in one of the best reconstituted primary recipients 12 weeks after transplant. On average, chimerism of GFP-positive cells was 41 to 83% in BM, 34 to 75.5% in spleen, 32 to 96.2% in thymus, 15 to 37.1% in lymph nodes, and 31 to 63% in the peritoneal cavity.

Reconstitution of GFP-positive cells in secondary recipients

To further confirm that the retrovirus was integrated in expanded long-term reconstituting cells after the FGF-1 culture, we performed secondary transplantation. Because the mice transplanted with retrovirus-transduced KSL cells showed very low engraftment levels 12 weeks after the primary transplantation, they were not subjected to secondary transplantation. Mice that had received FGF-1-expanded and retrovirus-transduced cells were sacrificed and GFP-positive cells from the BM were sorted. Again, 1×10^5 GFP-positive cells were injected into lethally irradiated secondary recipients (B6-Ly5.2 mice). All mice survived the transplantation. Unlike the primary transplantation in which cultured cells were injected, levels of chimerism in secondary recipients in the peripheral blood were lower at 4 weeks posttransplant in all lineages, but they reached values of 56 ± 7.3% in myeloid and 49 ± 7.6% in lymphoid lineages 8 weeks posttransplant. These levels were maintained at 12 weeks after the secondary transplantation (Fig. 5A). Multilineage reconstitution in the peripheral blood, BM, thymus, spleen, and lymph nodes by GFP-positive cells at 12 weeks after the secondary transplantation in a representative mouse is shown in Figure 5B and C. On average, the percentage of GFP-positive cells was 41 to 85% in BM, 32 to 63% in spleen, 24 to 75% in thymus, 12 to 33% in lymph nodes, and 40 to 63% in the peritoneal cavity. Representative multilineage reconstitution in different organs in a single mouse 12 weeks after the secondary transplantation is presented in Figure 6.

These results indicate that the FGF-1-expanded and subsequently retrovirus-transduced BM cells maintain full multilineage differentiation potential after the serial transplantation in vivo.

It appears that GFP expression levels slightly declined in secondary recipients (Figs. 4C and 5C). This suggests a decrease in the copy number of transgene or partial silencing of vector expression by methylation in serially transplanted HSCs.

Discussion

In this study, we present a method for highly efficient retrovirus transduction into mouse long-term reconstituting cells precultured for 3 weeks in vitro. This is a major challenge to the paradigm that freshly obtained HSCs are the best target for retrovirus-mediated gene transfer because of their presumed highest stem cell potential.

To enrich HSCs and to have them enter the cell cycle are the two major requisites for successful retroviral transduction. To these ends, in mouse HSC transduction, treatment of donor mice with 5-FU and/or antibody- or fluorescent dye-based cell sorting and cytokine treatment during the transduction period have been the most widely used methods in general protocols. In these methods, HSC division necessary for retrovirus transduction depends on selected combinations of exogenous cytokines during a short transduction period as well as in vivo HSC recovery (in the 5-FU strategy).

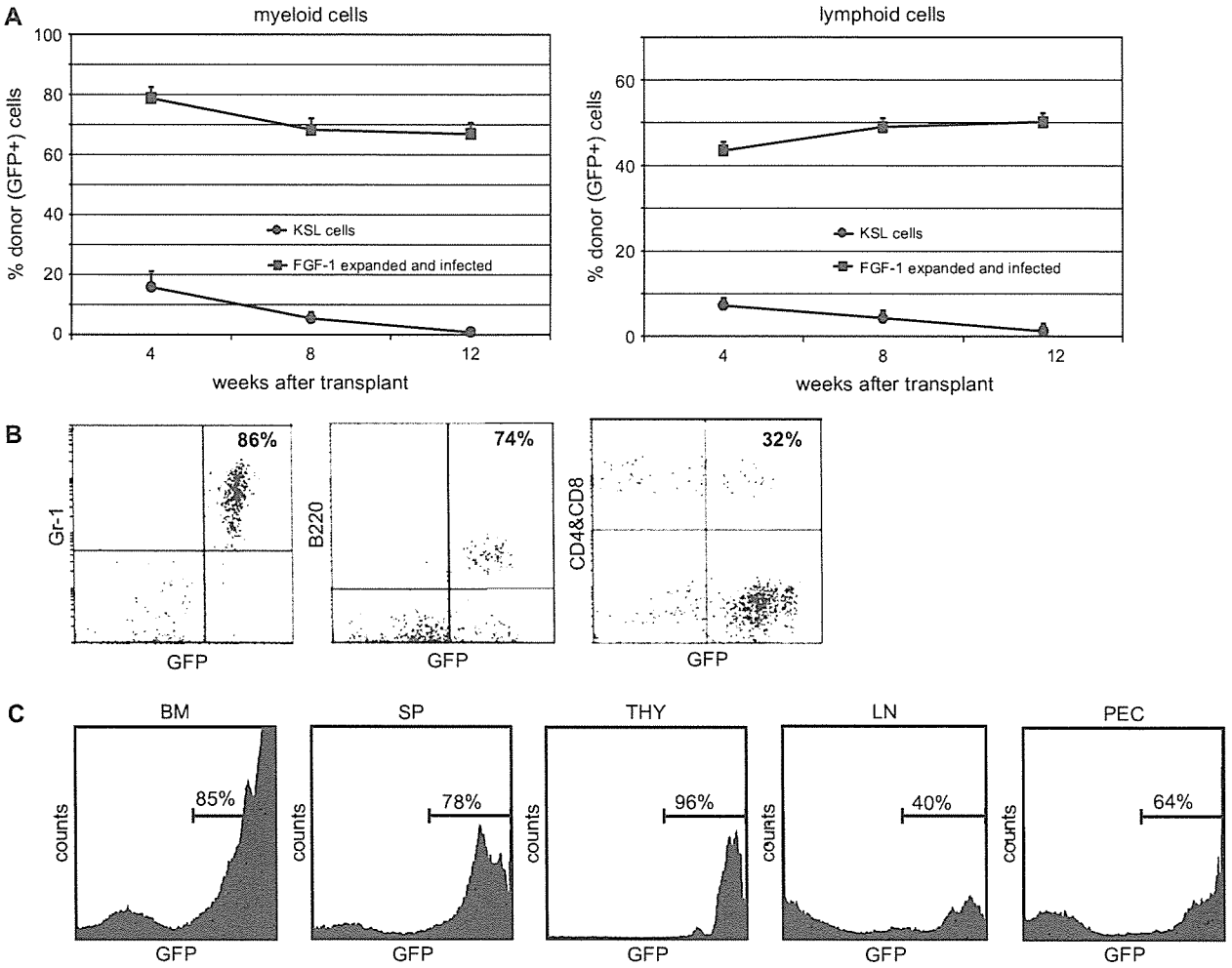

Figure 4. Contribution of GFP-positive cells in the recipient mice 12 weeks after primary transplantation. **(A):** A total of 1×10^5 GFP-positive cells derived from the FGF-1-expanded and retrovirus-transduced culture were transplanted into one group of lethally irradiated recipient mice. In parallel, 1000 GFP-positive KSL cells were transplanted into another group of mice (three to four mice per group were used and the experiment was repeated five times). Engraftment of donor-derived myeloid and lymphoid cells in the recipients at indicated time points after the transplantation is shown. Representative results are shown as the mean ± SD of 46 animals. **(B):** Multilineage reconstitution with GFP-positive cells from the FGF-1-expanded and transduced cells at 12 weeks posttransplant in a representative recipient. **(C):** Contribution of GFP-positive (FGF-1-expanded and transduced) cells in hematopoietic organs of a representative recipient. BM, bone marrow; SP, spleen; THY, thymus; LN, lymph node; PEC, peritoneal cavity.

The lineage-negative population is one of the most frequently used long-term reconstituting cell sources in the study of stem cell biology. However, as a target for retrovirus-mediated gene delivery to HSCs, the KSL population obtained from untreated mice was worse than the FGF-1-expanded population, as shown in Figure 4 and Table 1. The retrovirus transduction efficiency for KSL cells in our experiments appears to be rather lower than those reported by others. This could be biased by sorting of the GFP-positive cells prior to transplantation. Another possibility is that the KSL cells are more difficult to efficiently transduce with retrovirus in comparison to Lin^- or Lin^-Sca1^+ cells maintaining the long-term engraftment potential, as we previously showed [12].

Whole BM cells prepared from 5-FU-treated mice could also be evaluated. Based on our experience and on the literature, the average number of cells available from a single donor mouse is approximately 3×10^6, the transduction efficiency is 40 to 60%, and the CRU frequency is known to be 1/2000 [17,18]. Thus, the absolute number of CRUs that could harbor the retrovirus is estimated to be 600 to 900 per mouse. Comparing these numbers with the results of the limiting dilution study presented in this paper (i.e., actual recovery of 4200 virus-transduced CRUs per mouse), we show that the FGF-1-cultured cells for 3 weeks are a significantly better source of HSCs as a target of retrovirus transduction.

There is an additional advantage in FGF-1-cultured population as a target of gene delivery. Besides the quite high

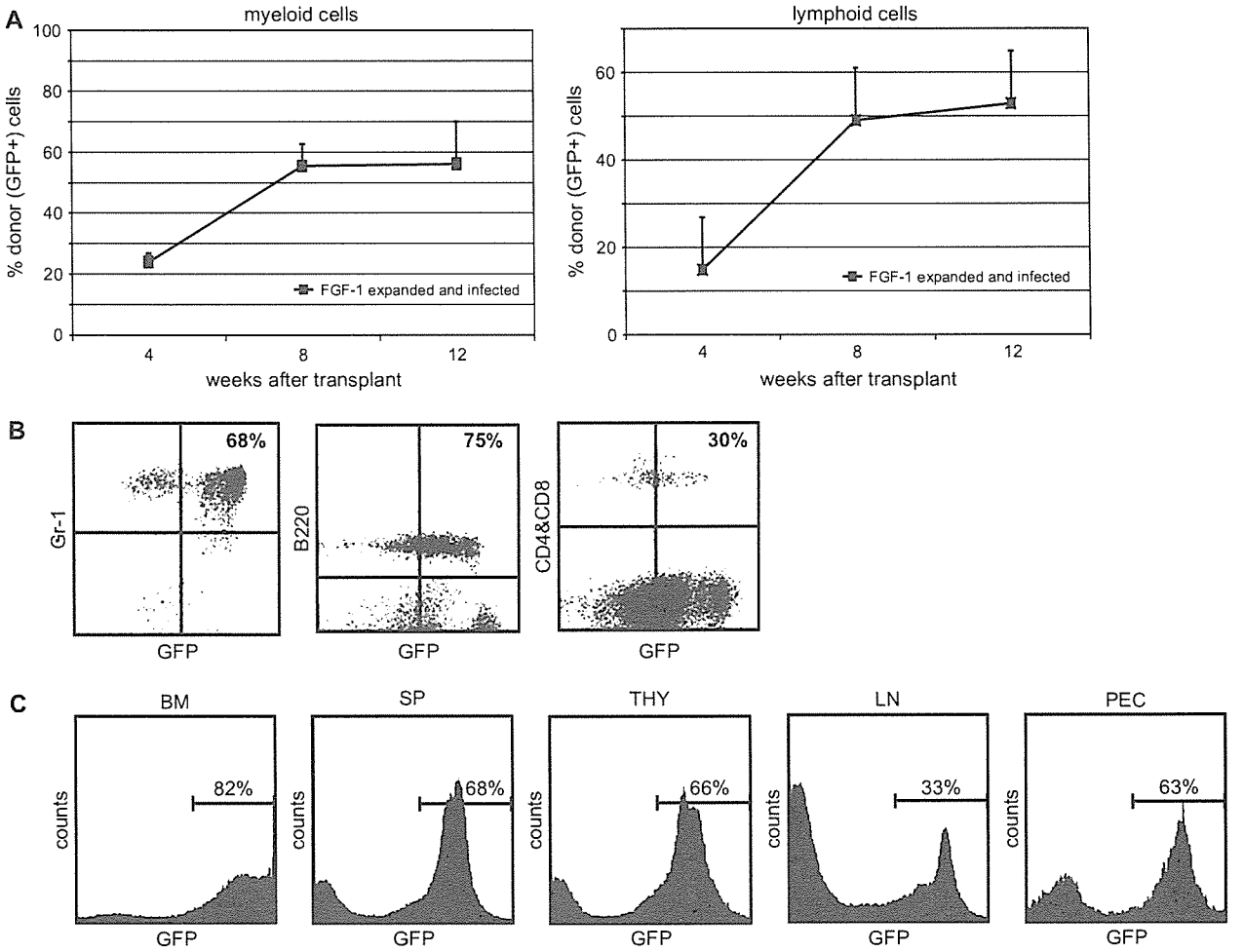

Figure 5. Reconstitution of GFP-positive cells in secondary recipients. A total of 1×10^5 GFP-positive cells were transplanted into lethally irradiated secondary recipients. Chimerism of the donor cells was checked in the peripheral blood of the recipient mice. Engraftment of donor-derived myeloid and lymphoid cells in the transplanted recipients at indicated time points after the transplantation is shown. Representative results are shown as the mean ± SD of 21 animals. **(B):** Multilineage reconstitution in the peripheral blood of a recipient mouse transplanted with GFP-positive cells. **(C):** Contribution of GFP-positive cells in hematopoietic organs of a representative secondary recipient. BM, bone marrow; SP, spleen; THY, thymus; LN, lymph node; PEC, peritoneal cavity.

long-term chimerism, we showed radiation protection and high short-term chimerism with 1×10^5 precultured retrovirus-transduced cells without any rescue cells. This is most likely due to the high ratio of progenitor cells in the FGF-1-expanded and retrovirus-transduced population. The higher short-term chimerism in primary recipients than in secondary ones offers additional support to this conclusion. This is particularly advantageous in experiments in which high chimerism from gene-delivered donor cells is needed. For example, to observe the rescue of the hematolymphopoietic phenotype in the gene knockout mice, this system confers an ideal source of cells for a number of experiments. Indeed, we could rescue a knockout phenotype in the hematopoietic compartment using the protocol described here (data not shown).

It is not completely elucidated in this article whether the quality of FGF-1-expanded HSCs is the same as that of freshly obtained HSCs from BM. In fact, we analyzed the primary recipients 10 weeks after transplant, which could be too short to assess whether the transplanted cells represented true long-term repopulating cells, according to the previous retroviral marking studies. However, we showed long-term and multilineage engraftment at fairly high chimerism levels not only in the primary but also in the secondary recipients. More extensive explorations may reveal similarities and differences between fresh and FGF-1-expanded HSCs.

The robust retroviral transduction of HSCs most probably stems from the expansion of HSCs during the preculture with FGF-1 before transduction. From this consideration, other HSC expansion methods could be chosen for retrovirus transduction protocols, such as the ones using Wnt3a [19,20], Notch ligands [21], and HoxB4 [22]. Compared to these, however, in which HSC purification was required,

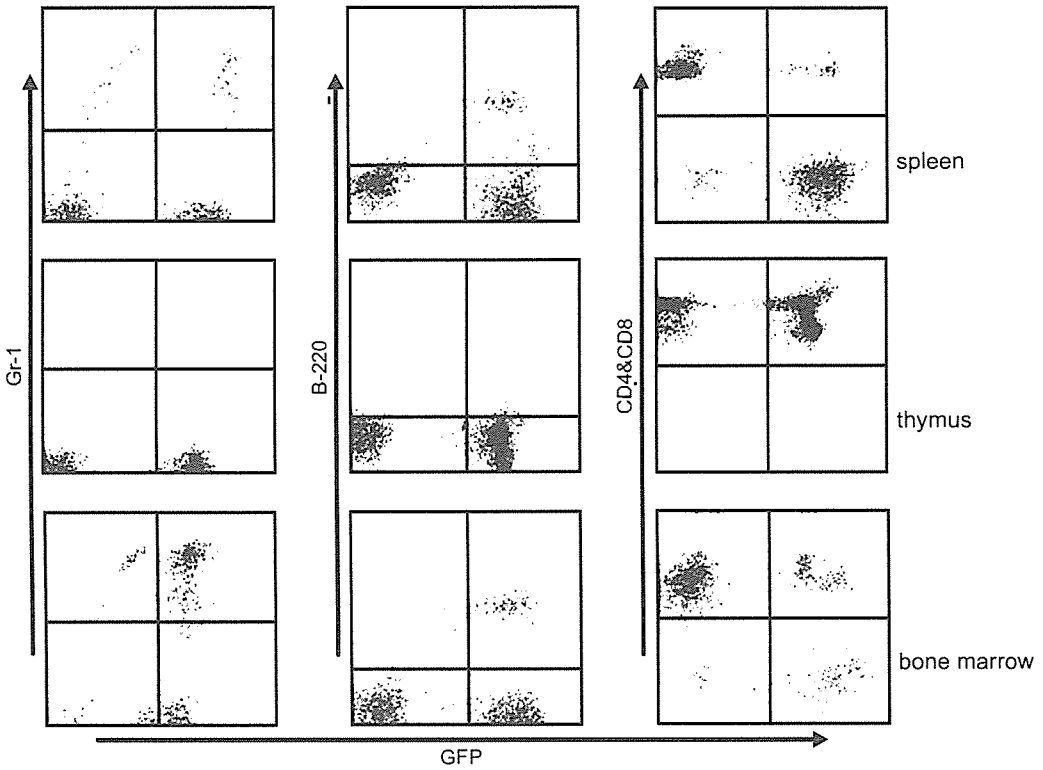

Figure 6. Multilineage reconstitution in secondary recipients. Multilineage reconstitution in the recipient mice was evaluated 12 weeks after the secondary transplantation. Reconstitution in different hematopoietic organs in a representative mouse is shown. bm, bone marrow; sp, spleen; thy, thymus. The cells from different organs were stained with Gr1 (for myeloid cells), B220 (for B cells), and CD4 and CD8 (for T cells). Engraftment of donor-derived granulocytes, B cells, and T cells is shown.

the method utilized here is unique in that we use whole BM cells without any purification, serving a very simple protocol. Moreover, FGF-1 is available on the market unlike Wnt3a or Notch ligands. Owing to this, it was easy to examine the reproducibility of HSC expansion by ourselves.

In our current experiments, MOI was calculated to be in the range between 300–340 and 1.1 to 1.2 $\times$ 10^4 for FGF-1-expanded and KSL cells, respectively. These values could be too high and may have yielded high transgene copy numbers [23]. It would be desirable to test the retroviral copy numbers; if they are high, we need to improve our gene transfer protocol.

The increase in the number of cells during the 3-day transduction period is possibly due to the preculture with FGF-1 together with heparin and to the combination of SCF, TPO, and FGF-1 without heparin during the transduction period. During this period, FGF-1 alone did not support cell growth nor virus transduction (Fig. 2A), and addition of other mitogenic cytokines such as the combination of SCF + TPO was required. This is probably due to the removal of the heparin, which is required to maximize the biologic activity of FGF-1, but on the other hand, its addition lowers the transduction efficiency [24].

Regarding the cytokines to be used during the transduction procedure, there is still no general agreement, and the use of a SCF + TPO combination was based on experience. Different research groups have reported diverse combinations [14,25]. The synergy between SCF and TPO has been reported [26–29], and our group has previously shown that this combination works well for retroviral transduction [11,30]. In the current protocol, FGF-1 was further added to that cytokine combination because it preserved the amount of KS cells slightly better than the combination without FGF-1 (Fig. 2B).

We did not examine whether the retrovirus-transduced HSCs were further expandable ex vivo, either in the presence of FGF-1 or supernatant in which the cells were grown. This is an interesting issue to be answered, particularly if the expansion efficiency is improved.

Consequently, the protocol introduced here using a retroviral vector for HSC gene transduction can be as efficient as protocols utilizing lentiviral vectors and superior to those with respect to the number of gene-transduced HSCs.

In conclusion, whole BM cells cultured in the presence of FGF-1 for 3 weeks provide HSCs highly competent to retrovirus transduction and can be of great value for the retrovirus-transduced HSC transplantation experiments.

Acknowledgments

A.C. is supported by a fellowship from the Ministry of Education, Culture, Sports, Science and Technology of Japan. This study was supported by Special Coordination Funds for Promoting Science and Technology from the Ministry of Education, Culture, Sports, Science and Technology of Japan, and Research on Pharmaceutical and Medical Safety, Health and Labor Sciences Research Grants from the Ministry of Health, Labor and Welfare of Japan. We express our deepest gratitude to Hisamaru Hirai, deceased in August, 2003. We also thank Toshio Suda and Fumio Arai of Keio University for their valuable discussions.

References

1. Conneally E, Cashman J, Petzer A, Eaves C. Expansion in vitro of transplantable human cord blood stem cells demonstrated using a quantitative assay of their lympho-myeloid repopulating activity in nonobese diabetic-scid/scid mice. Proc Natl Acad Sci U S A. 1997; 94:9836–9841.
2. Miller CL, Eaves CJ. Expansion in vitro of adult murine hematopoietic stem cells with transplantable lympho-myeloid reconstituting ability. Proc Natl Acad Sci U S A. 1997;94:13648–13653.
3. Zandstra PW, Conneally E, Petzer AL, Piret JM, Eaves CJ. Cytokine manipulation of primitive human hematopoietic cell self-renewal. Proc Natl Acad Sci U S A. 1997;94:4698–4703.
4. Bodine DM, McDonagh KT, Seidel NE, Nienhuis AW. Survival and retrovirus infection of murine hematopoietic stem cells in vitro: effects of 5-FU and method of infection. Exp Hematol. 1991;19:206–212.
5. Stewart FM, Crittenden RB, Lowry PA, Pearson-White S, Quesenberry PJ. Long-term engraftment of normal and post-5-fluorouracil murine marrow into normal nonmyeloablated mice. Blood. 1993;81:2566–2571.
6. de Haan G, Weersing E, Dontje B, et al. In vitro generation of long-term repopulating hematopoietic stem cells by fibroblast growth factor-1. Dev Cell. 2003;4:241–251.
7. Misawa K, Nosaka T, Morita S, et al. A method to identify cDNAs based on localization of green fluorescent protein fusion products. Proc Natl Acad Sci U S A. 2000;97:3062–3066.
8. Yoshimatsu T, Tamura M, Kuriyama S, Ikenaka K. Improvement of retroviral packaging cell lines by introducing the polyomavirus early region. Hum Gene Ther. 1998;9:161–172.
9. Miller AD, Buttimore C. Redesign of retrovirus packaging cell lines to avoid recombination leading to helper virus production. Mol Cell Biol. 1986;8:2895–2902.
10. Mann R, Mulligan RC, Baltimore D. Construction of a retrovirus packaging mutant and its use to produce helper-free defective retrovirus. Cell. 1983;1:153–159.
11. Osawa M, Hanada K, Hamada H, Nakauchi H. Long-term lymphohematopoietic reconstitution by a single 34-low/negative hematopoietic stem cell. Science. 1996;273:242–245.
12. Kunisato A, Chiba S, Nakagami-Yamaguchi E, et al. HES-1 preserves purified hematopoietic stem cells ex vivo and accumulates side population cells in vivo. Blood. 2003;101:1777–1783.
13. Lemischka IR, Raulet DH, Mulligan RC. Developmental potential and dynamic behavior of hematopoietic stem cells. Cell. 1986;45:917–927.
14. Pear WS, Miller JP, Xu L, et al. Efficient and rapid induction of a chronic myelogenous leukemia-like myeloproliferative disease in mice receiving P210 bcr/abl-transduced bone marrow. Blood. 1998; 92:3780–3792.
15. Antonchuk J, Sauvageau G, Humphries RK. HOXB4-induced expansion of adult hematopoietic stem cells ex vivo. Cell. 2002;109:39–45.
16. Varnum-Finney B, Xu L, Brashem-Stein C, et al. Pluripotent, cytokine-dependent, hematopoietic stem cells are immortalized by constitutive Notch1 signaling. Nat Med. 2000;6:1278–1281.
17. Szilvassy SJ, Humphries RK, Lansdorp PM, Eaves AC, Eaves CJ. Quantitative assay for totipotent reconstituting hematopoietic stem cells by a competitive repopulation strategy. Proc Natl Acad Sci U S A. 1990;87:8736–8740.
18. Szilvassy SJ, Lansdorp PM, Humphries RK, Eaves AC, Eaves CJ. Isolation in a single step of a highly enriched murine hematopoietic stem cell population with competitive long-term repopulating ability. Blood. 1989;74:930–939.
19. Reya T, Duncan AW, Ailles L, et al. A role for Wnt signalling in self-renewal of haematopoietic stem cells. Nature. 2003;423:409–414.
20. Willert K, Brown JD, Danenberg E, et al. Wnt proteins are lipid-modified and can act as stem cell growth factors. Nature. 2003;423:448–452.
21. Calvi LM, Adams GB, Weibrecht KW, et al. Osteoblastic cells regulate the haematopoietic stem cell niche. Nature. 2003;425:841–846.
22. Krosl J, Austin P, Beslu N, et al. In vitro expansion of hematopoietic stem cells by recombinant TAT-HOXB4 protein. Nat Med. 2003;11: 1428–1432.
23. Li Z, Schwieger M, Lange C, et al. Predictable and efficient retroviral gene transfer into murine bone marrow repopulating cells using a defined vector dose. Exp Hematol. 2003;31:1206–1214.
24. Carstanjen D, Dutt P, Moritz T. Heparin inhibits retrovirus binding to fibronectin as well as retrovirus gene transfer on fibronectin fragments. J Virol. 2001;75:6218–6222.
25. Srour EF, Abonour R, Cornetta K, Traycoff CM. Ex vivo expansion of hematopoietic stem and progenitor cells: are we there yet? J Hematother. 1999;8:93–102.
26. Sitnicka E, Lin N, Priestley GV, et al. The effect of thrombopoietin on the proliferation and differentiation of murine hematopoietic stem cells. Blood. 1996;87:4998–5005.
27. Ku H, Yonemura Y, Kaushansky K, Ogawa M. Thrombopoietin, the ligand for the Mpl receptor, synergizes with steel factor and other early acting cytokines in supporting proliferation of primitive hematopoietic progenitors of mice. Blood. 1996;87:4544–4551.
28. Ramsfjell V, Borge OJ, Veiby OP, et al. Thrombopoietin, but not erythropoietin, directly stimulates multilineage growth of primitive murine bone marrow progenitor cells in synergy with early acting cytokines: distinct interactions with the ligands for c-kit and FLT3. Blood. 1996; 88:4481–4492.
29. Ema H, Takano H, Sudo K, Nakauchi H. In vitro self-renewal division of hematopoietic stem cells. J Exp Med. 2000;192:1281–1288.
30. Kunisato A, Chiba S, Saito T, et al. Stem cell leukemia protein directs hematopoietic stem cell fate. Blood. 2004;103:3336–3341.

Host-Residual Invariant NK T Cells Attenuate Graft-versus-Host Immunity[1]

Kyoko Haraguchi,*† Tsuyoshi Takahashi,*[2] Akihiko Matsumoto,*† Takashi Asai,* Yoshinobu Kanda,*† Mineo Kurokawa,* Seishi Ogawa,*‡ Hideaki Oda,§ Masaru Taniguchi,¶ Hisamaru Hirai,[3]*† and Shigeru Chiba[4]*†

Invariant NK T (iNKT) cells have an invariant TCR-α chain and are activated in a CD1d-restricted manner. They are thought to regulate immune responses and play important roles in autoimmunity, allergy, infection, and tumor immunity. They also appear to influence immunity after hemopoietic stem cell transplantation. In this study, we examined the role of iNKT cells in graft-vs-host disease (GVHD) and graft rejection in a mouse model of MHC-mismatched bone marrow transplantation, using materials including α-galactosylceramide, NKT cells expanded in vitro, and Jα18 knockout mice that lack iNKT cells. We found that host-residual iNKT cells constitute effector cells which play a crucial role in reducing the severity of GVHD, and that this reduction is associated with a delayed increase in serum Th2 cytokine levels. Interestingly, we also found that host-residual iNKT cause a delay in engraftment and, under certain conditions, graft rejection. These results indicate that host-residual iNKT cells attenuate graft-vs-host immunity rather than host-vs-graft immunity. *The Journal of Immunology,* **2005, 175: 1320–1328.**

Natural killer T cells are a population of T cells that have NK cell markers such as NK1.1 (NKR-P1C) in mice or CD161 (NKR-P1A) in humans (1, 2). Some NK T cells use an invariant TCR-α chain (Vα14-Jα18 in mice, Vα24-Jα18 in humans) paired with Vβ8, Vβ7, or Vβ2 in mice or with Vβ11 in humans (3–7), and are called invariant NKT (iNKT)[5] cells. iNKT cells are activated by synthetic glycolipids such as α-galactosylceramide (α-GalCer) in a CD1d-restricted manner (1, 2, 8, 9). iNKT cells produce both Th1 (such as IFN-γ and TNF-α) and Th2 (such as IL-4, IL-5, IL-10, and IL-13) cytokines (1, 2, 8, 9). It has been reported that iNKT cells control immune responses in some infections, tumors, autoimmune diseases, and allograft rejection (1, 2, 8, 9).

Graft-vs-host disease (GVHD) is one of the most serious complications in hemopoietic stem cell transplantation. It has been suggested in a mouse acute GVHD model that NK1.1$^+$ T cells obtained from donor bone marrow can suppress GVHD induced by peripheral blood transplantation from the same donor (10). It has also been shown that a selected conditioning regimen, which preserves more host-residual NK1.1$^+$ or DX5$^+$ T cells than other T cells, is advantageous for reducing acute GVHD (11, 12). Furthermore, the suppressive effect of α-GalCer on induced acute GVHD has been demonstrated in a mouse model(13, 14). We previously reported that the number of iNKT cells was lower in patients with GVHD than in those without GVHD (15) after hemopoietic stem cell transplantation, although the cause-effect relationship was not clear.

In this report, we provide direct evidence that host-residual iNKT cells reduce GVHD in a mouse model of MHC-mismatched bone marrow transplantation using Jα18 knockout mice that lack iNKT cells (16). Adoptively transferred iNKT cells with grafts also reduce GVHD, but, importantly, this effect is dependent on the presence of host-residual iNKT cells.

Materials and Methods

Mice

C57BL/6 (H-2^b) and BALB/c (H-2^d) mice were purchased from Japan Clea. Jα18 knockout mice (16) were kindly provided by M. Harada (Chiba University, Chiba, Japan) and bred in the University of Tokyo animal facility. Drinking water for bone marrow transplant recipients was supplemented with 25 μg/ml neomycin sulfate and 0.3 U/ml polymyxin B (Sigma-Aldrich). Mouse studies were conducted according to the University of Tokyo Animal Experiment Manual.

Abs and reagents

The following Abs were purchased from BD Pharmingen: anti-CD4 (RM4-5), CD8α (53-6.7), CD45R/B220 (RA3-6B2), NK1.1 (PK136), H2D^b (KH95), H2D^d (34-2-12), I-A^b (AF6-120.1), I-A^d (39-10-8), LY-6G (Gr-1)/Ly6C (RB6-8C5), TCRβ(H57-597), and CD16/CD32 (2.4G2). α-GalCer was kindly provided by Kirin Brewery. Rabbit anti-asialo GM1 Ab was purchased from Wako Biochemicals. Murine rIL-7 and IL-15 were purchased from PeproTech. Human rIL-2 was kindly provided by Shionogi. Murine CD1d tetramer was established by Dr. M. Kronenberg (La Jolla Institute for Allergy and Immunology, La Jolla, CA) (17) and kindly provided by Dr. Nakayama (Chiba University, Chiba, Japan).

GVHD model

Six- to 8-week-old BALB/c hosts were given total-body irradiation (8 Gy) from a 150-Kv x-ray source and injected with donor cells via the tail vein within 6 h. All mice received 1 × 10^7 bone marrow cells and 1 × 10^7

Departments of *Hematology/Oncology, †Cell Therapy/Transplantation Medicine, and ‡Regeneration Medicine for Hematopoiesis, University of Tokyo Graduate School of Medicine and Hospital, Tokyo, Japan; §Department of Pathology, Tokyo Women's Medical University, Tokyo, Japan; and ¶RIKEN Research Center for Allergy and Immunology, Yokohama, Japan

Received for publication December 9, 2004. Accepted for publication April 21, 2005.

The costs of publication of this article were defrayed in part by the payment of page charges. This article must therefore be hereby marked *advertisement* in accordance with 18 U.S.C. Section 1734 solely to indicate this fact.

[1] **This work was supported in part by a Grant-in-Aid for Scientific Research,** KAKENHI (14370300), and Research on Regulatory Sciences of Pharmaceuticals and Medical Devices, Health and Labour Sciences Research Grants, Ministry of Health, Labour and Welfare of Japan.

[2] Current address: Division of Immunology & Rheumatology, Stanford University School of Medicine, Palo Alto, CA.

[3] Hisamaru Hirai died on August 23, 2003.

[4] Address correspondence and reprints requests to Dr. Shigeru Chiba, Department of Cell Therapy and Transplantation Medicine, University of Tokyo, 7-3-1 Hongo, Bunkyo-ku, Tokyo 113-8655, Japan. E-mail address: schiba-tky@umin.ac.jp

[5] Abbreviations used in this paper: iNKT, invariant NK T; α-GalCer, α-galactosylceramide; GVHD, graft-vs-host disease; CBA, cytometric bead array, cRPMI, complete RPMI.

0022-1767/05/$02.00

spleen cells obtained from C57BL/6 or BALB/c. Donor mice were 6–10 wk old and the same sex as the hosts. For α-GalCer treatment, mice received 2 μg/mouse (18, 19) α-GalCer, corresponding to ~100 μg/kg (20, 21), or control vehicle i.p. every 4 days from day 0 or −4 of transplantation. For the iNKT adoptive transfer model, mice received 1×10^6 in vitro-expanded iNKT cells with donor cells. For in vivo NK cell depletion, mice received 20 μl of rabbit anti-asialo GM1 Ab on days −5 and −1 or on day −1 of transplantation. We used the same amount of PBS as a control. Survival and appearance were monitored daily and body weight was measured every other day. GVHD was assessed by a scoring system that summed changes in five clinical parameters: weight loss, posture, activity, fur texture, and skin integrity (maximum index = 10) as previously described (22). Histopathological specimens from the skin, liver, and intestine of 15 dying mice were obtained on days 5–59 (median, 18 days) after transplantation and were stained with H&E.

Serum cytokines

Serum was obtained from recipient mice at 3- 6 h (early phase) or on day 5 or 6 posttransplant and stored at −20°C. IL-2, IL-4, IL-5, TNF-α, and IFN-γ were detected simultaneously using the mouse Th1/Th2 cytokine cytometric bead array (CBA) kit (BD Pharmingen).

In vitro stimulation of immunized splenocytes with α-GalCer

BALB/c mice were injected with α-GalCer (2 μg/mouse) or control vehicle i.p. and sacrificed 6 days after the injection. Splenocytes (1×10^5) were incubated with 100 ng/ml α-GalCer or control vehicle in RPMI 1640 medium supplemented with 10% FCS, penicillin-streptomycin, and 50 μM β-ME (complete RPMI (cRPMI)) for 72 h. The supernatants were collected and measured for the concentrations of cytokines using the mouse Th1/Th2 cytokine CBA kit.

Chimerism

We sacrificed mice on days 3–14 (median, 5 days) posttransplant. Splenocytes were stained with H-2D^b-FITC or H-2D^d-FITC, CD4-PE and CD8-allophycocyanin Abs. Bone marrow cells were stained with H-2D^b-FITC or H-2D^d-FITC and Gr-1-PE Abs. To analyze NKT chimerism, hepatic mononuclear cells were prepared as previously described (20) and stained with H-2D^b-FITC or H-2D^d-FITC, α-GalCer-loaded murine CD1d tetramer-PE and TCRβ-allophycocyanin Abs. Propidium iodine (BD Biosciences) was used to exclude dead cells. Immunofluorescence staining was performed according to standard procedures (15). Cells were analyzed by FACSCalibur and CellQuest software (BD Biosciences).

In vitro culture of iNKT cells

Vα14$^+$ NKT cells were established as follows. Thymocytes of 5- to 7-wk-old C57BL/6 and BALB/c mice were pretreated with anti-CD16/CD32 Abs to block FcγR and incubated with NK1.1-PE (C57BL/6) or α-GalCer-loaded CD1d tetramer (BALB/c), followed by anti-PE microbeads, and sorted by positive magnetic bead sorting (MACS; Miltenyi Biotec). Splenic dendritic cells were obtained in a standard procedure. In short, spleens were injected with 100 U/ml collagenase D (Roche Diagnostics) and minced. After the incubation in collagenase D for 45 min at 37°C, the spleen fragments were passed through a steel mesh and RBCs were lysed. The cells were cultured overnight in cRPMI with 30 ng/ml α-GalCer. Nonadherent cells were sorted by CD11c Microbeads (Miltenyi Biotec). NK1.1- or α-GalCer-loaded CD1d tetramer-positive thymocytes were cultured for 7 days with irradiated (15 Gy) α-GalCer-pulsed splenic dendritic cells in cRPMI supplemented with human IL-2 (30 U/ml), murine IL-7 (40 ng/ml), murine IL-15 (50 ng/ml), and α-GalCer (30 ng/ml).

In vitro cytokine production by cultured iNKT cells

For in vitro cytokine production assay, 5×10^4 Vα14$^+$ NKT cells and 5×10^4 α-GalCer-pulsed splenic dendritic cells were suspended in 200 μl of cRPMI and cultured in 96-well plates. After 24 h, the supernatants were collected from each well and assayed for the concentrations of cytokines using the mouse Th1/Th2 cytokine CBA kit.

Molecular analysis of TCR-α transcripts

Total RNA was extracted from 1×10^6 NKT cells according to the manufacturer's protocol (Tri Reagent LS; Sigma-Aldrich) and reverse transcribed. The transcribed cDNA was subjected to PCR amplification using the primer pair (5′-CTAAGCACAGCACGCTGCACA-3′, Vα14; and 5′-TGGCGTTG GTCTCTTTGAAG-3′, Cα) or the pair for β-actin (5′-GAGAGGGA AATCGTGCGTGA-3′ and 5′-ACATCTGCTGGAAGGTGGAC-3′) under the following conditions: 94°C for 60 s, 60°C for 60 s, and 72°C for 60 s for 40 cycles as described previously (7). For detection of the Vα-Jα sequence, the DNA band was excised from the agarose gel and DNA was extracted and purified according to the manufacturer's protocol (QIAquick Gel Extraction kit; Qiagen). Nucleotide sequences were determined by an ABI PRISM 310 Genetic Analyzer (Applied Biosystems). The primer used for sequencing was 5′-TGGCGTTGGTCTCTTTGAAG-3′.

Statistical analysis

Mouse survival was analyzed by the log-rank test. GVHD scores in the two groups were compared using repeated measures ANOVA. Differences in the proportion of iNKT cells and the chimerism were analyzed using Student's *t* test. The cytokine levels in serum were analyzed using the nonparametric Mann-Whitney *U* test. A $p < 0.05$ was considered to be significant.

Results

Establishment of GVHD model mice

In the prototype transplantation from wild-type C57BL/6 to wild-type BALB/c, all of the recipients showed lethal GVHD as judged by the GVHD score. Histological examinations also confirmed GVHD in representative mice (data not shown). In this setting, we confirmed that full donor chimerism was achieved in all of the recipients (data not shown). We performed all of the transplantation experiments two to four times independently, and integrated all of the results from individual experiments to avoid experiment-to-experiment variation.

Administration of α-GalCer prolonged survival of GVHD mice

First, we administered either α-GalCer to activate iNKT cells or control vehicle every 4 days from the day of transplantation. α-GalCer-treated mice survived significantly longer than control mice ($p < 0.0001$, Fig. 1*A*). The severity of GVHD in α-GalCer-treated mice was milder than that in control mice (Fig. 1*B*). The GVHD score within the first 30 days after transplantation in the two groups was compared by repeated measures ANOVA and was found to be significantly lower in the α-GalCer group ($p < 0.0001$).

We then examined whether α-GalCer treatment influenced the number of iNKT cells in the liver, which contains the largest proportion of iNKT cells (1, 9) (14.2 ± 4.7% in our measurements; Fig. 1*Di*), after transplantation. In control recipients, the ratio of iNKT cells to lymphocytes decreased rapidly and iNKT cells became undetectable by approximately day 5 posttransplant (Fig. 1, *C* and *D*). The rate of decrease in the iNKT cells was delayed in α-GalCer-treated mice, although iNKT cells were scarcely detectable after day 10 even in mice treated with α-GalCer (Fig. 1*C*). We observed temporary donor-type iNKT cell chimerism before the disappearance, although the time course of the donor:recipient iNKT cell ratio was highly variable (data not shown).

Interestingly, we found that the engraftment of donor CD4$^+$ T cells in α-GalCer-treated mice was delayed compared with that in control mice during the early phase after transplantation, although complete donor chimerism was eventually achieved (Fig. 2*A*). Engraftment of Gr-1$^+$ cells was also slightly delayed, but engraftment of other lineage cells was similar to that seen in vehicle-treated mice (data not shown). These findings encouraged us to compare various cytokine levels between α-GalCer-treated and control mice, since iNKT cells produce high levels of both Th1 and Th2 cytokines and could influence Th1/Th2 polarization. Therefore, we examined the serum levels of IFN-γ, TNF-α, IL-4, and IL-5 shortly after transplant and found that all of the cytokines were increased by α-GalCer treatment (Fig. 2*B*, *i-iv*), reproducing previous reports that α-GalCer has been shown to rapidly stimulate Th1 and Th2 cytokine production in vivo in the nontransplantation

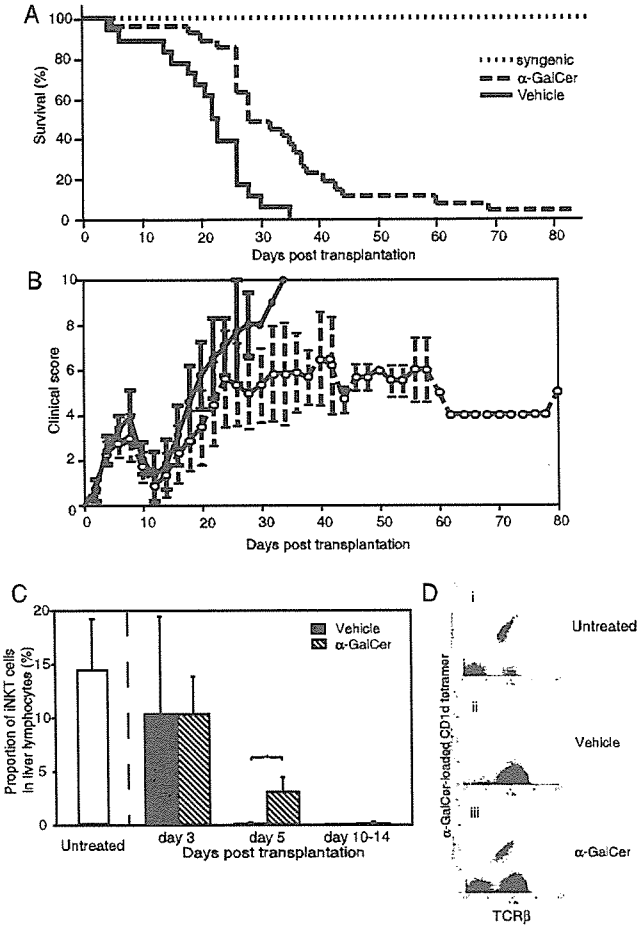

FIGURE 1. Survival of α-GalCer-treated GVHD mice. *A*, Survival of α-GalCer-treated (n = 27) mice, control vehicle-treated (n = 18) GVHD mice, and syngeneic cell-transplanted mice (n = 7). α-GalCer-treated GVHD mice survived longer than vehicle-treated GVHD mice ($p < 0.0001$). *B*, Mean clinical score and SD of α-GalCer-treated and vehicle-treated GVHD mice. The GVHD score was determined from the surviving mice shown in *A*. Within the first 30 days after transplantation, the GVHD score was significantly lower in the α-GalCer-treated group ($p < 0.0001$). *C*, Proportion of iNKT cells in liver lymphocytes from untreated mice and those early after transplantation. We analyzed liver iNKT cells from 6 vehicle- and 6 α-GalCer-treated recipients on day 3, 9 vehicle- and 11 α-GalCer-treated recipients on day 5, and 10 vehicle- and 10 α-GalCer-treated recipients on days 10–14 (median, 11 days). There is a statistically significant difference between the proportions of liver iNKT cells from vehicle- and α-GalCer-treated recipients on day 5 posttransplant ($p < 0.0001$). *D*, Representative FACS dot plots for liver iNKT cells from mice on day 5 posttransplant or an untreated mouse.

model (23–25). In contrast, it has been reported that in vivo α-GalCer-primed splenocytes secrete less amounts of Th1 cytokines after further in vitro treatment with α-GalCer compared with vehicle-primed splenocytes (23, 26). In our experimental system, we could exactly reproduce these findings (Fig. 2*C*, *i-iv*). Then we measured all four cytokines on day 5 or 6 posttransplant (1 or 2 days after the second α-GalCer administration), both in α-GalCer- and vehicle-treated mice. At this time point, GVHD signs were not been obvious yet, although the damage from radiation was inseparably measured "GVHD score" in Fig. 1*B*. IFN-γ and TNF-α levels in α-GalCer-treated mice were significantly lower than those in control mice, whereas levels of IL-4 and IL-5 in α-GalCer-treated mice were significantly higher in α-GalCer-treated mice (Fig. 2*D*, *i-iv*). These findings suggested that the administration of repeated α-GalCer somehow influenced cytokine production by iNKT cells, which resulted in a difference in the engraftment of donor $CD4^+$ T cells and a shift to the Th2 cytokine pattern early after transplantation.

iNKT adoptive transfer prolonged survival of GVHD mice

To obtain more direct evidence that the regulatory function of α-GalCer is mediated through iNKT cells, we first examined whether adoptively transferred iNKT cells attenuate GVHD. NK1.1- or α-GalCer-loaded CD1d tetramer-positive thymocytes from either C57BL/6 or BALB/c mice, respectively, were enriched and expanded in vitro. The purity of α-GalCer-loaded CD1d tetramer-positive cells after expansion was 90–98% (median, 95%) (Fig. 3*A*). To confirm that most of the in vitro-expanded NKT cells use the invariant TCR α-chain, we performed RT-PCR on RNA from the cells using the Vα14 and Cα primers and analyzed a fragment encompassing the V-J junction. The sequence of the RT-PCR product (Fig. 3*B*) was GCCACCTACATCTGGTGGT GGGCGATAGAGGTTCAGCCTTAGGGAGGCTGCATTTT, which is compatible with the sequence of the Vα14-Jα18 invariant chain. Furthermore, we checked in vitro function of expanded iNKT cells. Stimulation by autologous (or allogeneic, data not shown) dendritic cells in the presence of α-GalCer induced iNKT cells to produce a higher amount of cytokines compared with that in the presence of vehicle. This cytokine production was blocked by anti-CD1d Ab (Fig. 3*C*, *i-iv*).

These iNKT cells (1×10^6) were transferred along with the C57BL/6-derived graft (2×10^7) to irradiated BALB/c mice. As a control, the same amount (2×10^7) of C57BL/6-derived graft alone was used. The 5% difference in the total cell number was within the range of error. These recipient mice survived significantly longer than control mice, regardless of whether the adoptively transferred iNKT cells were derived from C57BL/6 or BALB/c mice ($p < 0.001$ Fig. 3*D*). To see whether transferred iNKT cells had expanded in the recipients, we examined iNKT cells in the liver lymphocytes. On days 5–7 posttransplant, there were very few iNKT cells in the liver of control mice that received grafts without adoptive iNKT cells (Fig. 3*Ei*). In contrast, iNKT cells were clearly detected on the same days in the liver of recipient mice that had been transplanted with grafts containing adoptive iNKT cells. This observation was independent of whether the transferred iNKT cells were derived from C57BL/6 or BALB/c mice (Fig. 3*E*, *ii-iii*). Surprisingly, if the origin of the adopted iNKT cells was the same as the donor strain (C57BL/6), both H-$2D^d$-negative (C57BL/6-derived) and H-$2D^d$-positive (BALB/c-derived) iNKT cells were reproducibly detected (Fig. 3*Ev*). Similarly, if the origin of the adopted iNKT cells was the same as the host strain (BALB/c), both BALB/c-derived and C57BL/6-derived iNKT cells were reproducibly detected (Fig. 3*Eiv*). The former result indicates that the adopted donor strain iNKT cells were temporarily engrafted and helped host-residual iNKT cells remain. The latter result indicates that the adopted host strain iNKT cells were engrafted or helped host-residual iNKT cells remain and further helped graft-contaminated iNKT cells be engrafted temporarily.

Then we measured serum cytokines shortly after transplantation with adoptive iNKT transfer. The serum cytokine levels in the iNKT-transferred mice were higher than those in the recipient mice without iNKT cell transfer. Therefore, iNKT cell transfer mimics the α-GalCer administration in the acute phase cytokine production profile in the recipient mice.